AD-A041 573 MICHIGAN UNIV ANN ARBOR DEPT OF AEROSPACE ENGINEERING F/G 20/4
UNSTEADY MOTION OF SHOCK WAVES IN TWO DIMENSIONAL TRANSONIC CHA--ETC(U)
JUN 77 T C ADAMSON, M S LIOU N00019-76-C-0435
UNCLASSIFIED 014534-F NL

1 OF 2
ADA041573

~~END~~ CONT.

DATE FILMED
8-77

UM 014534-F

Unsteady Motion of Shock Waves in Two Dimensional Transonic Channel Flows

(12)

T. C. ADAMSON JR.
M. S. LIOU

June 1977

Final Technical Report
Prepared for
Naval Air Systems Command
Washington, D.C. 20361
Contract N00019-76-C-0435

Department of Aerospace Engineering

SECURITY CLASSIFICATION OF THIS PAGE (When Data Entered)

REPORT DOCUMENTATION PAGE		READ INSTRUCTIONS BEFORE COMPLETING FORM
1. REPORT NUMBER UM 014534-F	2. GOVT ACCESSION NO.	3. RECIPIENT'S CATALOG NUMBER
4. TITLE (and Subtitle) Unsteady Motion of Shock Waves in Two Dimensional Transonic Channel Flows		5. TYPE OF REPORT & PERIOD COVERED Final Technical Report 15 May 1976 - 15 June 1977 6. PERFORMING ORG. REPORT NUMBER
7. AUTHOR(s) T. C. Adamson, Jr. and M. S. Liou		8. CONTRACT OR GRANT NUMBER(s) N00019-76-C-0435
9. PERFORMING ORGANIZATION NAME AND ADDRESS Department of Aerospace Engineering The University of Michigan Ann Arbor, Michigan 48109		10. PROGRAM ELEMENT, PROJECT, TASK AREA & WORK UNIT NUMBERS
11. CONTROLLING OFFICE NAME AND ADDRESS Naval Air Systems Command Code AIR-310 Washington, D.C. 20361		12. REPORT DATE June 1977 13. NUMBER OF PAGES 64 pages
14. MONITORING AGENCY NAME & ADDRESS (if different from Controlling Office) 68p.		15. SECURITY CLASS. (of this report) Unclassified 15a. DECLASSIFICATION/DOWNGRADING SCHEDULE

16. DISTRIBUTION STATEMENT (of this Report)

APPROVED FOR PUBLIC RELEASE:
DISTRIBUTION UNLIMITED

17. DISTRIBUTION STATEMENT (of the abstract entered in Block 20, if different from Report)

18. SUPPLEMENTARY NOTES

19. KEY WORDS (Continue on reverse side if necessary and identify by block number)

Unsteady transonic flow, compressible channel flow, shock waves

20. ABSTRACT (Continue on reverse side if necessary and identify by block number)

Two dimensional unsteady transonic channel flow with a shock wave is considered for the so-called slowly varying time regime. Solutions are studied for two specific cases within this general time regime, the cases corresponding to small and large amplitude shock wave motions. For the large amplitude case, conditions are considered under which the shock wave →

next page

DD FORM 1 JAN 73 1473 EDITION OF 1 NOV 65 IS OBSOLETE

402 605

SECURITY CLASSIFICATION OF THIS PAGE (When Data Entered)

cont → travels upstream of the throat, disappears, and then reforms at the throat. A unified solution which covers both cases is developed. Numerical results are presented. A short discussion of shock induced separation in unsteady flows is given.

UNSTEADY MOTION OF SHOCK WAVES IN TWO DIMENSIONAL TRANSONIC CHANNEL FLOWS

by

T. C. Adamson, Jr.
M. S. Liou

Department of Aerospace Engineering
The University of Michigan

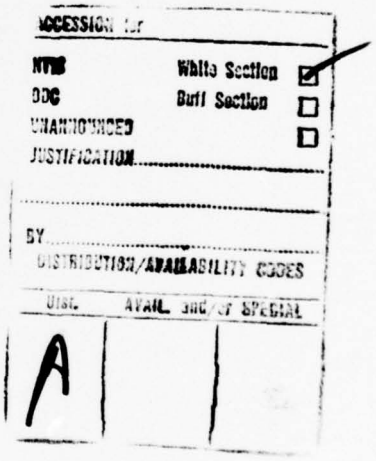

Final Technical Report

prepared for

Naval Air Systems Command
Washington, D.C. 20361
Contract N00019-76-C-0435

June 1977

(I) INTRODUCTION

Transonic channel flows have applications in most modern high performance jet engines. Because the blades in a rotor rotate past fixed vanes, and because of various disturbances caused by combustion instabilities, flow asymmetries, etc., these flows are inherently unsteady. Since the flow is transonic, small changes in pressure downstream of a shock wave, can cause large variations in the position of the shock wave and thus large variations in forces on the blades.

Previous work on unsteady two dimensional channel flows with shock waves[1], [2] indicates that a great many physical problems of interest fall in the so called slowly varying time regime. If $\bar{T}_{ch}$ is the characteristic time associated with an impressed pressure oscillation, say, (overbars denote dimensional quantities) and $\bar{L}$ and $\bar{a}^*$ are the channel throat half width and critical sound speed respectively, then this region is characterized by the relation

$$\bar{T}_{ch} / \left(\frac{\bar{L}}{\bar{a}^*} \right) \gg 1;$$

That is, the period associated with the impressed oscillation is large compared to the time taken by an acoustic wave to cross the channel. As pointed out in reference 1, for typical conditions in a jet engine,

---

[1] Richey, G. K. and Adamson Jr., T. C., "Analysis of Unsteady Transonic Channel Flow with Shock Waves," AIAA Journal, 14, 1976, pp. 1054-1061.

[2] Messiter, A. F. and Adamson Jr., T. C., "Asymptotic Solutions for Nonsteady Transonic Channel Flows," Symposium Transsonicum II, Eds., Oswatitsch, K. and Rues, D., Springer Verlag, 1976, pp. 41-48.

this "slowly varying" time regime encompasses a range of frequencies ($\bar{f} = \bar{T}_{ch}^{-1}$ = cycles/sec) of $100 < \bar{f} < 1000$. This frequency range is evidently of considerable interest.

Within the general condition $\bar{T}_{ch}/(\bar{L}/\bar{a}^{*}) \gg 1$ there are two specific cases of physical interest in flows with shock waves. They have to do with the comparison of the characteristic time associated with the impressed pressure oscillations, $\bar{T}_{ch}$, with the characteristic time for a signal to travel from the point where the oscillation is introduced downstream of the shock wave to the shock wave itself, say $\bar{T}_{sh}$. Thus, if

(1) $\dfrac{\bar{T}_{ch}}{\bar{T}_{sh}} = O(1)$ — pressure signals from downstream reach the shock wave in a time comparable with the time characterizing the pressure variation (e.g., the period of the pressure oscillations). Oscillations in velocity, pressure, etc., in the channel flow downstream of a shock wave lag behind the impressed pressure oscillations.

(2) $\dfrac{\bar{T}_{ch}}{\bar{T}_{sh}} \gg 1$ — pressure signals from downstream reach the shock wave "instantaneously" compared to the time characterizing the pressure variation. Oscillations in velocity, pressure, etc.,

in the channel flow downstream of a shock wave are in phase with the pressure oscillations.

The remaining order, $\bar{T}_{ch}/\bar{T}_{sh} \ll 1$, appears to be a more complicated and probably less important version of case (1), and is not considered here. Case (1) is considered in reference (1) for a symmetric channel. In reference (2), solutions are presented for case (1) written in terms of unsteady boundary conditions rather than initial conditions; in addition, the concepts inherent in case (2) are discussed briefly and the differential equation describing the instantaneous shock wave position in a channel with parabolic walls is derived for a particular case in which the impressed disturbances have a sinusoidal time dependence. In both references, solutions are given in terms of asymptotic expansions; thus, the type of solution first postulated by Szaniawski[3] for steady transonic flows are derived in a systematic manner and extended to cover unsteady flows.

In this report, solutions for case (1) are reviewed and numerical solutions for a typical case are given. Next, detailed solutions for case (2) are presented, again with numerical results for a typical case. Finally, a general solution, (case (3)), which holds for either case, is presented, with an error estimate which allows one to make

---

[3] Szaniawski, A., "Transonic Approximations to the Flow Through a Nozzle," Archiwum Mechaniki Stosowanej, 17, 1965, pp. 79-85.

simplifications in the numerical calculations on a systematic basis, i.e., on the basis of a desired accuracy. A detailed description of the various possible shock wave motions for periodic impressed pressure oscillations is also presented. All results are given for symmetric channels.

Finally, a discussion of the use of steady flow predictions of shock induced separation to predict separation in unsteady flows is given.

(II) UNSTEADY TRANSONIC CHANNEL FLOWS WITH SHOCK WAVES

The problem considered is that of a two dimensional channel with an arbitrary wall shape, in which there is a transonic flow with a shock wave. A sketch of the channel flow illustrating the notation used, is shown in figure 1. The flow upstream of the wave is steady; pressure oscillations are impressed upon the flow downstream of the shock, at $x = X$, say, causing the shock wave position to oscillate. The gas is assumed to follow the perfect gas law and to have constant specific heats. The flow upstream of the shock wave is isentropic, and because the flow is transonic, the shock is weak enough that a velocity potential may be used to the order desired. The coordinates, x and y, are made dimensionless with respect to $\bar{L}$, the time, T, with respect to $\bar{L}/\bar{a}^*$, and velocities with respect to $\bar{a}^*$; hence, the dimensionless velocity potential is referred to the product $\bar{L}\bar{a}^*$. The pressure, P, density, ρ, and temperature, $\tilde{T}$, are made dimensionless with respect to their critical values, and the enthalpy is referred

to $\bar{a}^{*2}$.

The wall shapes considered are written as follows, for symmetric channels:

$$y_w = \pm (1 + \epsilon^2 f(x)) \tag{1}$$

where f(x) is the arbitrary wall shape function, such that $f(0) = f'(0) = 0$. Thus, x is measured from the channel throat. The radius of curvature of the channel, at the throat, is $O(\epsilon^{-2})$ from eqn. (1), and as will be seen later, $u-1 = O(\epsilon)$. Hence, for transonic flow, $\epsilon \ll 1$.

Unsteady flows may be characterized by prescribing the relative order of the characteristic time associated with the impressed disturbances, $\bar{T}_{ch}$, and the characteristic time associated with the acoustic waves traveling through the channel, $\bar{L}/\bar{a}^*$. As mentioned previously, the so called slowly varying time regime is considered here, where $\bar{T}_{ch} \gg \bar{L}/\bar{a}^*$. Therefore, a parameter, τ, is introduced and the time is stretched, as follows:

$$\tau \equiv \bar{T}_{ch}/(\bar{L}/\bar{a}^*) \qquad T = \tau t \tag{2a, b}$$

so that $\tau \gg 1$ and $t = O(1)$. The relationship between τ and ϵ depends on which of the cases mentioned previously is considered. Again, $\bar{T}_{sh}$ is the order of the time it takes a signal to travel upstream from the origin of the flow disturbance to the shock wave, a distance of order $\bar{L}$, say. A disturbance pulse travels upstream at sonic velocity relative to the flow and thus at an absolute dimensionless velocity, $u_p = 1-u = O(\epsilon)$. Hence, $\bar{T}_{sh} = O(\bar{L}/\bar{a}^* u_p) = O(\bar{L}/\bar{a}^* \epsilon)$, and $\bar{T}_{ch}/\bar{T}_{sh} = O(\tau/\epsilon)$. Therefore, it is seen that case (1) mentioned

previously and considered in reference (1) is that for which $\tau = O(\epsilon^{-1})$, and case (2) is that for which $\tau \gg \epsilon^{-1}$, and here we choose $\tau = O(\epsilon^{-2})$. In summary, then, we consider the following two cases.

$$\text{Case (1)} \qquad \tau_1 = (k_1 \epsilon)^{-1} \tag{3a}$$

$$\text{Case (2)} \qquad \tau_2 = (k_2 \epsilon^2)^{-1} \tag{3b}$$

where k_1 and k_2 are arbitrary constants of order unity.

In the following, solutions are presented in the form of asymptotic expansions, uniformly valid to order ϵ^2. Although the method is valid for more general impressed disturbances, attention here is focused on oscillatory second order pressure fluctuations impressed on the flow downstream of the shock wave. Upstream of the shock wave, the flow is steady.

Solutions for Case (1), $\tau_1 = (k_1 \epsilon)^{-1}$

The solutions for Case (1), derived in reference (1), may be written as follows:

$$u = 1 + \epsilon u_1 + \epsilon^2 u_2 + \ldots \tag{4a}$$

$$v = \epsilon^2 v_2 + \ldots \tag{4b}$$

$$P = 1 - \epsilon\gamma u_1 - \epsilon^2 \gamma u_2 + \ldots \tag{4c}$$

$$\rho = 1 - \epsilon u_1 - \epsilon^2 (u_2 + (\frac{\gamma-1}{2})\ u_1^2) + \ldots \tag{4d}$$

$$\tilde{T} = 1 - \epsilon(\gamma-1)u_1 - \epsilon^2(\gamma-1)(u_2 + \frac{u_1^2}{2}) + \ldots \tag{4e}$$

where $\gamma = C_P/C_v$ is the ratio of specific heats, and where

$$u_1 = \pm \sqrt{\frac{2}{(\gamma+1)} f(x) + C_w} \tag{5a}$$

$$u_2 = f'' \frac{y^2}{2} + h_x + \zeta^*_{x^*} \tag{5b}$$

$$v_2 = f' y + \zeta^*_{y} \tag{5c}$$

$$\zeta^* = \frac{4f''_0 [(\gamma+1)C_u]^{1/2}}{\pi^3} \sum_{n=1}^{\infty} \frac{(-1)^n}{n^3} \exp\{-n\pi x^* / [(\gamma+1)C_u]^{1/2}\} \cdot \cos(n\pi y) \tag{5d}$$

$$x^* = (x - x_o)\epsilon^{-1/2} \tag{5e}$$

$$h_x = -\frac{1}{6}[f'' + (2\gamma-3)u_1^2] + \frac{c_2}{u_1} + \frac{1}{u_1} G(t-t_\ell) \tag{5f}$$

$$t_\ell = t_\ell(x) = \int_X^x (2k_1/(\gamma+1)u_1(\xi))d\xi \tag{5g}$$

Finally, the shock wave location is

$$x_s = x_0 + \epsilon\, x_{s1}(t) + \ldots \tag{6}$$

where x_0 is the steady state location, and x_{s1} is found from the equation,

$$\frac{4k_1}{(\gamma+1)} \frac{dxs_1}{dt} = h_{x_d} + h_{x_u} + \frac{f''_0}{3} - C_u^2 \tag{7a}$$

$$t = T/\tau_1 \tag{7b}$$

The y dependence of x_s occurs first in a term of order $\epsilon^{3/2}$. (1) In eqn. (5a), C_w is an arbitrary constant set by the value of the velocity at the throat; i.e., if the flow is supersonic or subsonic there, $C_w > 0$, while if the flow is one which accelerates from subsonic to supersonic flow, $C_w = 0$. Also, in eqns. (5), $f' = df/dx$, etc., and f'_0 is the derivative of f evaluated at x_0, C_u is the value of u_1 at x_0

evaluated upstream of the shock (upper sign in eqn. (5a)), C_2 is an arbitrary constant of integration set by boundary conditions, and G(t) is the oscillation in pressure impressed downstream of the shock wave at x = X, say. Hence, upstream of the shock wave, the equation for h_x would be found from eqn. (5f) by setting G = 0. In eqns. (5f) and (5g), $t_\ell = t_\ell(x)$ is the lag time, representing the time taken by a signal to travel upstream from x = X, to any position x. The subscripts u and d in eqn. (7a) indicate functions evaluated immediately upstream and downstream of the shock wave, respectively; thus, for example, $C_u = u_{1u}$ and from the shock jump conditions

$$u_{1d} = - C_u \tag{8}$$

The function $\zeta^*(x^*, y)$ in eqns.(5) is the additional velocity potential needed to make the solutions uniformly valid to order ϵ^2. That is, the solutions with $\zeta^* = 0$ are the outer solutions, which do not satisfy the shock wave jump conditions to second order. Hence, an inner region enclosing the shock wave must be considered. In this inner region, which has an extent of order $\epsilon^{1/2}$ so that the inner x-direction coordinate, x^*, is written as in eqn. (5e), it is found that the outer solutions do hold upstream of the shock wave, but that a new solution is necessary downstream of the shock wave. This new inner solution satisfies the shock jump conditions at $x^* = 0$ and matches with the downstream outer solution as $x^* \to \infty$. The inner and outer solutions are then joined to form a composite solution uniformly valid to order ϵ^2. Thus, upstream of the shock wave $\zeta^*_{x^*} = \zeta^*_y = 0$ in eqns. (5b) and (5c), while $\zeta^*_{x^*}$ and ζ^*_y are found from eqn. (5d) downstream of the shock.

Numerical solutions are carried out for given functional forms for the wall shape, $f(x)$, and impressed pressure distribution, $G(t)$, and for given values of γ, ϵ, τ, and the steady state pressure at $x = X$. Again, $x = X$ is the point at which a given pressure is impressed upon the flow; setting a given steady state pressure there sets x_0, the steady state shock location, and prescribing $G(t)$ there allows calculation of the corresponding nonstationary shock wave location. It should be noted that variations of pressure of order ϵ^2 at $x = X$, are sufficient to cause variations in shock location and thus pressure variations of order ϵ in the region in which the shock wave travels. This point is illustrated in figure 2, where a typical pressure distribution for an accelerating flow has been sketched.

Example calculations are shown in figures 3 and 4 for the following conditions:

$$
\begin{aligned}
f(x) &= 18x^2/13 && x \leq 1 \\
&= 27(x-2)^4/13 + 48(x-2)^3/13 + 3 && 1 \leq x \leq 2 \\
&= 3 && x > 2 \qquad (9) \\
G(t) &= 3 \sin(2t) && t \geq 0 \\
&= 0 && t < 0
\end{aligned}
$$

$$
\epsilon = 0.1 \qquad \gamma = 1.4 \qquad C_{2d} = -2\gamma C_u^3/3
$$

$$
\tau = 20 \qquad C_w = 0 \qquad X = 3 \qquad C_{2u} = 0
$$

The flow is taken to be an accelerating flow which goes through sonic velocity at the throat. Hence $C_w = 0$ and $C_{2u} = 0$. For $C_{2u} = 0$, satisfaction of the shock jump conditions demands that $C_{2d} = -2\gamma C_u^3/3$;

giving a numerical value for C_{2d}, then, is equivalent to setting the pressure at x = X and sets x_0, the shock location. That is, if

$$-\frac{2\gamma C_u^3}{3} = -\frac{2\gamma}{3}\left[\frac{2}{\gamma+1} f(x_0)\right]^{3/2} = -4.8323 \qquad (10)$$

then, using the equations given for f(x) in equations (9), one can show that $x_0 = 1.5$. Finally, for the given values for τ and ϵ, it is seen from eqn. (3a) that $k_1 = 2$. With these parameters known, eqns. (4) - (7) may be used to calculate velocity, pressure, temperature, and density distributions, and shock wave location and velocity, where

$$u_s = \frac{dx_s}{dT} = k_1\epsilon^2 \frac{dx_{s1}}{dt} + \ldots \qquad (11)$$

It should be noted that the wall shape shown in eqn. (9), was chosen so that f(x), f'(x), and f''(x) are continuous throughout the channel.

Isotachs and pressure distributions at the centerline and at the wall, at given times, are shown in figures 3a - 3f for the case where the flow is steady until, at time t = 0, the pressure oscillation indicated in eqn. (9) is started at x = X. It is seen that as the disturbance propagates upstream, the velocity profiles downstream of the shock change, and at time t = 0.39456 the disturbance reaches the shock and the shock position begins to change. The farthest forward position of the shock wave occurs at t = 1.96536, figure 3f.

Centerline pressure distributions corresponding to three different shock locations and thus to several different times are shown in figure 4. The shock is located at its farthest downstream location, $x = x_0 = 1.5$, until t = 0.39456; thus only the pressure distribution

downstream of x = 1.5 varies with time as illustrated by the two distributions at t = 0 and t = 0.39456. As the shock begins to move upstream, the fluid velocity relative to the wave, $u_u - u_s$, increases because the increase in $-u_s$, the shock wave velocity in the direction of the throat, is greater than the decrease in u_u, the steady state velocity upstream of the shock wave, caused by the decrease in the cross-sectional area of the channel. Hence the pressure jump across the shock increases, as indicated by the distribution marked t = 1.17996, where $x_s \cong 1.38$. At the farthest upstream shock location, indicated by the distribution market t = 1.96536, the shock velocity is zero. Finally, as the shock moves downstream and again reaches $x_s \cong 1.38$, at t = 2.75075, the fluid velocity relative to the shock wave is less than the steady state velocity at that point. Hence, the pressure jump across the shock and indeed the pressure at any point downstream of the wave, is less than the pressure at the corresponding point for the t = 1.17997 distribution when the wave was advancing. In figure 4, it should be noted that the fact that several of the pressure distributions have common points at x = 3, is fortuitous.

In figure 5, the shock wave position and velocity are shown as functions of time, for this sample case.

Solutions for Case (2), $\tau_2 = (k_2 \epsilon^2)^{-1}$

The fundamental ideas underlying the method of solution for this case were discussed briefly in reference (2). Here, detailed solutions are given for the same general problem considered for the case (1)

calculations. That is, unsteady flow with shock waves, in a two dimensional channel, is considered. The unsteadiness arises as the result of oscillations impressed on the flow at some point downstream of the shock; upstream of the shock, the flow is steady. The impressed oscillations again have an amplitude of order ϵ^2, i.e. they occur in the second order pressure. Now, however, the period of the oscillation is large compared to the time taken for a signal to travel upstream to the shock wave.

Because $\tau_2 \gg \tau_1$, and the partial derivative with respect to time is ordered by τ^{-1} (i.e., $\partial/\partial T = \frac{1}{\tau}\ \partial/\partial t$), it is clear that insofar as the general form of the outer solutions for u, v, P, etc., are concerned, the solutions for case (2) should be derivable from those for case (1), by simplification. Thus, eqns. (4), (5a), and eqns. (5b) and (5c) with $\zeta^* = 0$, hold for this case also. The questions which remain, then, are those concerning the calculations in the inner region, for ζ^*, the calculations for h_x, and the calculations for the shock wave position.

In case (1), because unsteady oscillations in pressure (and thus u) are impressed only in second order, the first order solution downstream of the shock has to be the steady subsonic solution associated with sonic flow at the throat, i.e., $u_1 = -\sqrt{\frac{2}{(\gamma+1)}\ f(x)}$ $(C_w = 0)$, since it would have to hold for the case where no shock exists, as indicated in figure 2. Between the throat and the shock, on the other hand, $u_1 = \sqrt{\frac{2}{\gamma+1}\ f(x)}$. Hence $u_{1d} = -u_{1u}$. As a result of these considerations, the shock velocity must be of order ϵ^2. That is, the shock wave jump condition relative to the wave is, to first order,

$$u_{1d} - u_{1s} = -(u_{1u} - u_{1s}) \tag{12}$$

where u_{1s} is the first order shock velocity. Since $u_{1d} = -u_{1u}$, it is seen that $u_{1s} = 0$, i.e. the shock velocity is of second order. Since $\tau_1 = O(\epsilon^{-1})$, then, the shock velocity, u_s, is

$$u_s = \frac{dX_s}{dT} = k_1 \epsilon \frac{dX_s}{dt} = k_1 \epsilon \frac{d}{dt}(x_0 + \epsilon x_1 + \ldots) \tag{13}$$

so that x_o must be constant, and $x_{s1} = x_{s1}(t)$. In the present case, for the reasons mentioned above, the shock wave velocity is, again, of order ϵ^2. However, $\tau_2 = O(\epsilon^{-2})$, so

$$u_s = \frac{dX_s}{dT} = k_1 \epsilon^2 \frac{dX_s}{dt} \tag{14}$$

and we see that now x_s varies with t in zeroth order. That is, the variation in shock position may be of order unity; the shock can move completely through the channel, as opposed to case (1) where the shock motion is a perturbation about a steady state location, x_0. Here, for convenience, we again write the steady state shock wave location as x_0 and write for the general shock location,

$$x_s = x_{so} + \epsilon x_{s1} + \ldots = x_0 + \Delta x_{so} + \epsilon x_{s1} + \ldots \tag{15}$$

Again, the y dependence of the shock shape is of higher order than that retained in eqn. (15).

Because the outer solutions do not satisfy the shock jump conditions to second order, it is necessary to consider an inner region enclosing the shock wave, just as in case (1).[1] However, the situation in this case is complicated by the fact that the shock wave moves over distances of order unity. That is, in case (1), because the shock motion

is a perturbation about x_0, with the order of the distance moved small compared to the thickness of the inner region, it is possible to consider a stationary inner region, inside which there is a higher order shock wave motion. Here, on the other hand, one must consider an inner region on a coordinate system which moves at the shock wave velocity; in view of the expansion for x_s, eqn. (15), it is sufficient to consider a coordinate system moving at the velocity $\dot{x}_{so} = dx_{so}/dT$.

If quantities relative to the moving coordinate system are denoted by a caret, then,

$$\hat{x} = x - x_{so} \qquad \hat{y} = y \qquad \hat{T} = T \qquad \hat{t} = t \qquad (16a, b, c, d)$$

$$\hat{\vec{q}} = \vec{q} - \vec{i}\,\dot{x}_{so} \qquad \hat{u} = u - \dot{x}_{so} \qquad \hat{v} = v \qquad (16e, f, g)$$

$$\hat{h}_t = h + \frac{\hat{q}^2}{2} = h_t - \hat{u}\,\dot{x}_{so} - \frac{\dot{x}_{so}^2}{2} \qquad (16h)$$

where $\hat{\vec{q}}$ is the vector velocity and $\hat{h}_t$ the stagnation enthalpy in the moving coordinate system; $h_t = h + q^2/2$, and $\vec{q}$ are the stagnation enthalpy and velocity in the absolute systems respectively, and h is the static enthalpy.

Since the moving system is a linearly accelerating system, the conservation equations may be derived from those valid in an inertial system by using the simple transformations,

$$\frac{\partial}{\partial T} = \frac{\partial}{\partial \hat{T}} - \dot{x}_{so}\frac{\partial}{\partial \hat{x}} \qquad \frac{\partial}{\partial x} = \frac{\partial}{\partial \hat{x}} \qquad \frac{\partial}{\partial y} = \frac{\partial}{\partial \hat{y}} \qquad (17a, b, c)$$

Thus, the mass, momentum, and energy conservation equations become

$$\frac{\partial \rho}{\partial \hat{T}} + \hat{\nabla} \cdot \rho\,\hat{\vec{q}} = 0 \qquad (18a)$$

$$\frac{\partial \vec{\hat{q}}}{\partial \hat{T}} + (\vec{\hat{q}} \cdot \hat{\nabla})\vec{\hat{q}} = -\frac{1}{\rho\gamma}\hat{\nabla}P - \vec{i}\,\ddot{x}_{so} \tag{18b}$$

$$\frac{\partial \hat{h}_t}{\partial \hat{T}} + \vec{\hat{q}} \cdot \hat{\nabla}\hat{h}_t + \hat{u}\ddot{x}_{so} = \frac{1}{\gamma\rho}\frac{\partial P}{\partial \hat{T}} \tag{18c}$$

Also, the following dimensionless property relations hold for a perfect gas with constant specific heats:

$$h = \frac{\tilde{T}}{\gamma-1} \tag{19a}$$

$$\rho = \tilde{T}^{\frac{1}{\gamma-1}} e^{-\Delta s} \tag{19b}$$

$$P = \rho\,\tilde{T} \tag{19c}$$

where s is the specific entropy made dimensionless with respect to R, the gas constant. If we now write the velocity as

$$\vec{\hat{q}} = \hat{\nabla}\hat{\Phi} + \vec{\hat{q}}_a \tag{20}$$

Then, using eqns. (18c) and (19), one can show that the energy equation can be written as

$$\vec{\hat{q}} \cdot \hat{\nabla}(\hat{h}_t + \hat{\Phi}_T + \hat{x}\,\ddot{x}_{so}) = -\frac{P}{\gamma\rho}\frac{\partial \Delta s}{\partial T} - \vec{\hat{q}} \cdot \frac{\partial \vec{\hat{q}}_a}{\partial T} \tag{21}$$

where $\hat{u}\ddot{x}_{so} = \vec{\hat{q}} \cdot \vec{i}\,\ddot{x}_{so} = \vec{\hat{q}} \cdot \nabla\hat{x}\,\ddot{x}_{so}$. Now, the Reynolds number is taken to be large enough that viscous effects are negligible, and the flow is transonic so that shock waves are weak (i.e., $\Delta s = O(\epsilon^3)$). If one writes the equation expressing the change in vorticity along a streamline in the moving coordinate system, one can thus show that $\hat{q}_a = O(\epsilon^{7/2})$. Moreover, since $\tau_2 = O(\epsilon^{-2})$, it is easy to show that the terms on the right hand side of eqn. (21) are negligible; that is to the

order desired, eqn. (21) becomes,

$$\hat{h}_t + \hat{\Phi}_{\hat{T}} + \hat{x}\,\ddot{x}_{so} = \hat{F}(\hat{T}) \tag{22}$$

This is the form of the Bernoulli equation to be used in the moving coordinate system. The corresponding equation in the inertial frame is[4]

$$h_t + \Phi_T = F(T) \tag{23}$$

The relationship between $F(T)$ and $\hat{F}(\hat{T})$ is easily found by writing equation (22) in terms of absolute quantities, using equations (16), (17), and the relation between Φ and $\hat{\Phi}$, i.e.

$$\Phi = \hat{\Phi} + \dot{x}_{so}\hat{x} \tag{24}$$

and by replacing $h_t + \Phi_T$ by $F(T)$ according to eqn. (23). The result is,

$$F(T) + \frac{\dot{x}_{so}^2}{2} = \hat{F}(\hat{T}) \tag{25}$$

Actually, since $\dot{x}_{so}^2 = k_2^2\epsilon^4 (d\,x_{so}/dt)^2 = O(\epsilon^4)$, $F(T) = \hat{F}(\hat{T})$ to the order desired. The values of $F(T)$ and $\hat{F}(\hat{T})$ upstream of the shock wave can be found easily by noting that there the flow is steady, so $\Phi_T = 0$, and F = constant evaluated in the undisturbed flow. Thus

$$F_u(T) = \hat{F}_u(\hat{T}) - \frac{\dot{x}_{so}^2}{2} = \frac{(\gamma+1)}{2(\gamma-1)} \tag{26}$$

The values of F and $\hat{F}$ downstream of the wave may be determined by noting that the stagnation enthalpy relative to the shock wave, written

---

[4] Guderley, K. G., The Theory of Transonic Flow, Pergamon Press, Addison-Wesley, 1962, p. 7.

either in inner or outer variables, is conserved across the wave, i.e. $\hat{h}_{td} = \hat{h}_{tu}$, where the subscripts u and d refer to positions immediately upstream and immediately downstream of the wave, respectively. Then, using eqns. (16), one can show that, therefore,

$$h_{td} - u_d \dot{x}_{so} + \frac{\dot{x}_{so}^2}{2} = h_{tu} - u_u \dot{x}_{so} + \frac{\dot{x}_{so}^2}{2} \tag{27}$$

and if, again, we let $C_u = u_{1u}(x_{so})$ and note that from the first order solutions, across the shock, $u_{1d} = -u_{1u}$, then eqn. (27) becomes,

$$h_{td} = \frac{\gamma+1}{2(\gamma-1)} - 2\epsilon \dot{x}_{so} C_u + \ldots \tag{28}$$

where $h_{tu} = \frac{(\gamma+1)}{2(\gamma-1)}$ and $u = 1 + \epsilon u_1 + \ldots$ have been used. Now, since the unsteady terms in the outer, inertial frame, solutions are of second order, and $\tau_2 = O(\epsilon^2)$, it is seen that downstream of the wave, $\Phi_T = O(\epsilon^4)$. Hence, to order ϵ^3 (since $\dot{x}_{so} = k_2 \epsilon^2 d\, x_{so}/dt$), one finds from eqns. (23) and (25) that

$$F_d(T) = \hat{F}_d(T) - \frac{\dot{x}_{so}^2}{2} = \frac{\gamma+1}{2(\gamma-1)} - 2\epsilon \dot{x}_{so} C_u + \ldots \tag{29}$$

Hence, the Bernoulli equations in the moving coordinate system, eqn. (22), and in the stationary coordinate system, eqn. (23), are known, both upstream and downstream of the shock wave, by virtue of eqns. (26) and (29). It should be noted that the same results are found if detailed inner region calculations are carried out.

An inner region, enclosing the shock wave, must be considered because, as mentioned previously, the outer solutions do not satisfy the shock jump conditions in second order. In this thin inner region,

then, the solutions must (i) match with the outer solutions term by term as the outer region is approached in an appropriate limit, (ii) satisfy the wall boundary conditions, and (iii) satisfy the shock jump condition at the shock wave. The analysis differs from that followed in reference (1) only in a few minor instances, so a very brief review is given here, with emphasis on the those differences.

The gas dynamic equation in the moving coordinate system may be derived from eqns. (18), (19), and (20), with $\vec{q}_a = 0$ and $\Delta s = 0$ (to the order desired here). However, it is simpler to transform the equation written in terms of absolute quantities,[4] using eqns. (17) and (24). The result is,

$$(a^2 - \hat{\Phi}_{\hat{x}}^2)\hat{\Phi}_{\hat{x}\hat{x}} + (a^2 - \hat{\Phi}_{\hat{y}}^2)\hat{\Phi}_{\hat{y}\hat{y}} - 2\hat{\Phi}_{\hat{x}}\hat{\Phi}_{\hat{y}}\hat{\Phi}_{\hat{x}\hat{y}} - \hat{\Phi}_{\hat{T}\hat{T}} - 2\hat{\Phi}_{\hat{x}}\hat{\Phi}_{\hat{x}\hat{T}} - 2\hat{\Phi}_{\hat{y}}\hat{\Phi}_{\hat{y}\hat{T}} - \ddot{x}_{so}\hat{\Phi}_{\hat{x}} - \dddot{x}_{so}\hat{x} + \dot{x}_{so}\ddot{x}_{so} = 0 \tag{30}$$

Just as in case (1)[1], it can be shown that the inner region is of order $\epsilon^{1/2}$ in thickness. Hence, inner variables are written as follows:

$$x^* = (x - x_{so})\epsilon^{-1/2} \qquad y^* = y \qquad T^* = T = \tau_2 t = \tau_2 t^* \tag{31a, b, c}$$

and an inner velocity potential may be defined as

$$\Phi^*(x^*, y^*, T^*) = \epsilon^{-1/2}\hat{\Phi}(\hat{x}, \hat{y}, \hat{T}) = x^*(1 - \dot{x}_{so}) + \epsilon^{-1/2}x_{so} + \phi^*(x^*, y^*, t^*) \tag{32}$$

where ϕ^* is the perturbation potential. From eqns. (31) and (32), it is seen that

$$\hat{u} = \hat{\Phi}_{\hat{x}} = \Phi^*_{x^*} = u^* = 1 + \phi^*_{x^*} - \dot{x}_{so} \tag{33a}$$

$$\hat{v} = \hat{\Phi}_{\hat{y}} = \epsilon^{1/2}\Phi^*_{y^*} = \epsilon^{1/2}v^* = \epsilon^{1/2}\phi^*_{y^*} \tag{33b}$$

The matching conditions for u^* and v^*, i.e. the solutions to which they should match as $x^* \to \pm\infty$, are found by transforming the outer solutions for u and v (eqns. (4), (5a), (5b), and (5c) with $\zeta^* = 0$) into velocities in the moving coordinate system, $\hat{u}$ and $\hat{v}$ (eqns. (16f) and (16g)), then expanding these solutions about x_{so} and writing the resulting expressions in inner variables. If $\dot{x}_{so}$ is subtracted from eqn. (31a) in reference (1), then eqns. (31) in that reference are precisely the desired relations. Now in case (1), because x_0 = constant was the zeroth order shock wave position, no further matching was required. Here, because $x_{so} = x_{so}(t)$, there is a function of time in the potential which must be found, in order to evaluate $\Phi^*_{I^*}$ properly in the inner region counterpart of eqn. (22), the Bernoulli equation. This term is found by matching the potential; i.e. using eqns. (24) and(32), with $\Phi = x + \epsilon\phi_1 + \epsilon^2\phi_2 + \ldots$, and expanding $\hat{\Phi}$ about x_{so}, one can show that the inner perturbation potential, ϕ^*, must approach

$$\phi^*(\pm\infty, y^*, t^*) = \epsilon^{1/2}\phi_1(x_{so}) + \ldots \tag{34}$$

where $\phi_1(x_{so})$ has its value downstream of the shock for the upper sign in ϕ^*, and its value upstream of the shock for the lower sign. Finally, the resulting expansion for ϕ^* is,

$$\phi^* = \epsilon^{1/2}\phi_1(x_{so}) + \epsilon\phi^*_1 + \epsilon^{3/2}\phi^*_{3/2} + \epsilon^2\phi^*_2 + \ldots \tag{35}$$

where, since $x_{so} = x_{so}(t)$, then $\phi_1(x_{so})$ is a function of time alone, and,

$$\phi^*_{t^*} = \frac{dx_{so}}{dt}\,\phi_{1x}(x_{so}),$$

with $\phi_{1x}(x_{so}) = C_u$ upstream of the shock and $\phi_{1x}(x_{so}) = -C_u$ downstream of the shock. It should be noted that in case (2), $C_u = C_u(t)$ since $x_{so} = x_{so}(t)$.

With the expansion for ϕ^* known, the governing equation in the inner region may be derived. Thus, eqn. (22), with

$$\hat{h}_t = h + \frac{\hat{u}^2+\hat{v}^2}{2} = \frac{a^2}{\gamma-1} + \frac{\hat{u}^2+\hat{v}^2}{2} \tag{36}$$

is used for a^2 in eqn. (30), and the resulting equation, using eqns. (3b) (31), (32), and (35), is written in terms of inner variables; finally, governing equations for each ϕ_i^* may be written. These equations are precisely the same as those derived for case (1), because even though $u_{1u}(x_{so}) = C_u$ is not a constant, and in fact is a function of time, there are no time derivatives involved in the governing equations to the order desired, as a result of the order of τ_2. Also, the boundary conditions at the wall and the shock jump conditions are unchanged. Hence, the inner region solutions are the same as those given in reference (1); that is, one can define an added second order potential function, ζ^*, in the same way and obtain for it the same solution. Therefore, eqns. (4), and (5a) - (5f) give a composite general solution for u and v, uniformly valid to second order, for case (2) as well as case (1). There remains only the question of the proper forms for h_x and the shock position, corresponding to eqns. (5f) and (7a) respectively, in case (2).

The equation for h_x, which occurs in the second order outer solution for u, is found by deriving the third order velocity solutions

and applying the boundary conditions. The procedure follows exactly those steps given in reference (1) and so will not be repeated here. The equation found for h_x is, then, for case (2),

$$h_x = -\frac{1}{6}(f'' + (2\gamma-3)u_1^2) + \frac{A(t)}{u_1} \tag{37}$$

where A(t) is a function of integration. This is the same equation found for h_x in case (1)[1] except that in case (1), an additional term, h_t, appears in the equation. Because $\tau_2 \gg \tau_1$, and $\partial h/\partial T = \frac{1}{\tau}(\partial h/\partial t)$, it is clear that in case (2) the term $\partial h/\partial t$ appears in a higher order calculation rather than in the same equation as h_x; hence in case (2), the calculation for h_x is easier than in case (1). The boundary condition to be applied, in order to evaluate A(t), is that a given, unsteady, pressure is impressed downstream of the flow, say at x = X, these pressure oscillations being in second order, as stated earlier. Now, since one can write the pressure as[1],

$$P = 1 - \epsilon\gamma u_1 - \epsilon^2 \gamma u_2 + \ldots \tag{38}$$

and since the unsteady part of u_2 is $h_x(x,t)$, it is clear that a condition on h_x is equivalent to a condition on the second order pressure; hence boundary conditions on h_x are given downstream of the wave.

For steady flow, A(t) is a constant, say c_2, so

$$h_x = -\frac{1}{6}(f'' + (2\gamma-3)u_1^2) + \frac{C_2}{u_1} \tag{39}$$

Thus, eqn. (39) holds upstream where the flow is steady, and where $C_2 = C_{2u}$, say. Downstream of the shock, where the flow may be

unsteady, it is convenient to write h_x as the sum of a steady term, $(h_x)_{ss}$, given by eqn. (39), and an unsteady contribution, $\tilde{h}_x$, where, then

$$\tilde{h}_x(x,t) = \frac{A(t)-C_2}{u_1} \tag{40}$$

If the boundary condition is written as

$$\tilde{h}_x(X,t) = \frac{G(t)}{u_1(X)} \tag{41}$$

Then it is seen that $A(t) - C_2 = G(t)$ and so in general,

$$h_x = -\frac{1}{6}(f'' + (2\gamma-3)u_1^2) + \frac{C_2}{u_1} + \frac{G(t)}{u_1} \tag{42}$$

When this solution is compared with the corresponding solution for case (1), given by eqn. (5f), it is seen that the only difference is the absence of the time lag in G, in eqn. (42). This, of course, arises as a result of the fact that in the present case $\bar{T}_{ch} \gg \bar{T}_{sh}$, so that in the limit as $\epsilon \to 0$, there is no time lag; the impressed pressure oscillations and the corresponding oscillations in u, P, ρ, etc., are in phase.

The equation for the shock wave location is found by applying the mass conservation principle to a control volume containing the shock wave, and hence attached to the moving coordinate system. If this control volume is considered to have an extent, in the flow direction, of order $\epsilon^{1/2}$ (the control volume extends from a constant negative value of x^* to a constant positive value of x^*), then the variation with time of the mass within the control volume is at least of order $\epsilon^{7/2}$. Since the interest here is only in terms to and including $O(\epsilon^3)$, the time variation

term need not be considered, and so conservation of mass demands that

$$\left[\int_0^{\hat{y}_w} \rho\,\hat{u}\,d\hat{y}\right]_u = \left[\int_0^{\hat{y}_w} \rho\,\hat{u}\,d\hat{y}\right]_d \tag{43}$$

where, from eqns. (4), (5), (16), (19), (22), (29), (32), and (36),

$$\rho\,\hat{u} = 1 - \epsilon^2\left(\left(\frac{\gamma+1}{2}\right)u_1^2 + k_2\dot{x}_{so}\right) - \epsilon^3\left(\frac{\Delta s}{3} + k_2 C_u \dot{x}_{so} - \frac{(\gamma+1)(3-2\gamma)}{6}u_1^3\right.$$
$$\left. + (\gamma+1)u_1\left(f''\frac{y^2}{2} + h_x + \zeta^*_{x^*} - k_2\dot{x}_{so}\right) + (\gamma-1)u_1 k_2\dot{x}_{so}\right) + \ldots \tag{44}$$

Upstream of the wave, $u_1 = C_u$ and $\zeta^*_{x^*} = 0$, while downstream of the wave, $u_1 = -C_u$ and $\zeta^*_{x^*}$ is calculated using eqn. (5d) and evaluated at some $x^* =$ constant. In both locations, $f'' = f''(x_{so}) + \ldots = f''_{so}$, say. Finally $\Delta s = s - s_u = 0$ upstream of the wave and is equal to the Δs across a weak shock[5] downstream of the wave, i.e.

$$(s_d - s_u) = \epsilon^3\,\frac{2\gamma}{3}\,(\gamma+1)C_u^3 + \ldots \tag{45}$$

Since we are interested only in terms up to $O(\epsilon^3)$, and $\hat{y}_w = 1 + O(\epsilon^2)$, it is seen from eqns. (43) and (44) that in the integral in eqn. (43), the limit $\hat{y}_w$ may be replaced by 1. Now, if eqn. (44) is substituted into eqn. (43), using the above mentioned substitutions upstream and downstream of the wave, then from the first nonzero term ($O(\epsilon^3)$), it is found that since $\int_0^1 \zeta^*_{x^*} dy^* = 0$,

---

[5] Liepmann, H. W. and Roshko, A., Elements of Gasdynamics, John Wiley and Sons, 1957, p. 60.

$$\frac{4k_2}{(\gamma+1)} \frac{dx_{so}}{dt} = h_{x_d} + h_{x_u} + \frac{f''_{so}}{3} - C_u^2 \qquad (46)$$

Thus, the form is exactly that found for case (1), eqn. (7a). However, in eqn. (46), C_u and f''_{so}, for example, are functions of time rather than being constants as in eqn. (7a); as will be seen, this leads to differences in shock wave velocity between the two cases.

It should be noted at this point that the general form of the solution is the same for the two cases. The differences, which are fundamental, are in the details of the solution, i.e., in case (1) a time lag, t_ℓ, is involved and in case (2) it is not, and in case (1) functions evaluated at the shock are constant, while in case (2) they are functions of time.

Before showing example numerical calculations for case (2), it is of interest to write equation (46) in a more convenient form and compare it with its counterpart from case (1). The problem considered is, again, that of a flow which accelerates through sonic velocity at a throat. There is a shock wave in the flow, which is steady until, at time $t = 0$, second order pressure oscillations are impressed upon the flow downstream of the shock wave. If eqn. (42) is used to calculate h_{x_d} and h_{x_u}, then, since $C_{2u} = 0$, eqn. (46) becomes,

$$\frac{4k_2}{(\gamma+1)} \frac{dx_{so}}{dt} = -\frac{1}{C_u}\left[C_{2_d} + \frac{2\gamma}{3} C_u^3 + G(t)\right] \qquad (47)$$

Equations (5f) and (7a) may be used to derive the corresponding equation for case (1). Thus,

$$\frac{4k_1}{(\gamma+1)} \frac{dx_{s1}}{dt} = -\frac{1}{C_{uo}} \left[C_{2_d} + \frac{2\gamma}{3} C_{uo}^3 + G(t-t_{\ell o}) \right] \tag{48}$$

where $t_{\ell o} = t_\ell(x_o)$ (see eqn. (5g)), and where $C_{uo} = C_u(x_o)$. At steady state, when $G = 0$ and $\frac{dx_{so}}{dt} = 0 = \frac{dx_{s1}}{dt}$, both eqns. (47) and (48) give,

$$C_{2_d} = -\frac{2\gamma}{3} C_u^3(x_o) = -\frac{2\gamma}{3} C_{uo}^3 \tag{49}$$

so that finally, one can write, for eqns. (47) and (48), where, again, $C_u = u_1(x_{so})$,

$$\frac{4k_2}{(\gamma+1)} \frac{dx_{so}}{dt} = \frac{1}{C_u} \left(\frac{2\gamma}{3} (C_{uo}^3 - C_u^3) - G(t) \right) \tag{50a}$$

$$\frac{4k_1}{(\gamma+1)} \frac{dx_{s1}}{dt} = -\frac{1}{C_{uo}} G(t-t_{\ell o}) \tag{50b}$$

The differences between the two shock motions are apparent, when written in this form. A more detailed discussion of the shock motion for case (2), eqn. (47) or eqn. (50a), is given later.

Numerical solutions for a typical case (2) flow are shown in figures 3a ($t=0$, steady state), 6a to 6c, and 7. The wall shape, functional form of G(t), and in fact all parameters except for τ are the same as those used in the numerical examples shown for case (1), figures 3 to 5 (Eqns. 9). Thus, in Case (2), $\tau_2 = 100$ while in case (1), $\tau_1 = 20$. The most significant difference noted between the two cases is the overall shock wave motion.

Unified Solutions - Case (3)

The differences between the two cases considered are very clear from an asymptotic viewpoint. However, if one wishes to make flow field computations for a given set of physical constants, the choice of which set of solutions to use is not so clear. Thus, if $\epsilon = 0.1$ and $\tau = 40$, then should one use case (1) solutions with a $k_1 = .25$ or case (2) solutions with $k_2 = 2.5$? A relatively simple answer to this question consists of using the results of the previous analysis to write a unified solution for numerical computations.

From the preceding analysis, it is clear that the general form of the solution for case (1) is the same as that for case (2). In what follows, the aim is to write a solution which reduces properly to either case. We first rewrite the time lag, eqn. (5g), as follows:

$$t_\ell = \frac{1}{\tau\epsilon} \int_X^x \frac{2}{(\gamma+1)} \frac{d\xi}{u_1(\xi)} \tag{51}$$

Then as $\tau \to \tau_1 = (k_1\epsilon)^{-1}$, eqn. (51) reduces to eqn. (5g), and as $\tau \to \tau_2 = (k_2\epsilon^2)^{-1}$, $t_\ell = O(\epsilon)$, and becomes negligibly small. The unified solution thus is written with $G(t-t_\ell)$ in h_x, with t_ℓ given by eqn. (51).

The only remaining difference is that in the equations for the shock wave velocity, i.e., eqns. (47) and (48). For the unified solution, we write

$$x_s = x_0 + x_s^+(t) \tag{52a}$$

$$\frac{1}{\tau\,\epsilon^2}\,\frac{4}{(\gamma+1)}\,\frac{dx_s^+}{dt} = -\frac{1}{C_u}\left[C_{2d} + \frac{2\gamma}{3}C_u^3 + G(t-t_{\ell o})\right] \tag{52b}$$

$$t_{\ell o} = \frac{1}{\tau\,\epsilon}\int_X^{x_o} \frac{2}{(\gamma+1)}\,\frac{d\xi}{u_1(\xi)} \tag{52c}$$

and for the specific problem considered here, where oscillations are impressed on a flow with a steady state shock location, $C_{2d} = -2\gamma C_{uo}^3/3$ and so eqn. (52b) becomes:

$$\frac{1}{\tau\,\epsilon}\,\frac{4}{(\gamma+1)}\,\frac{dx_s^+}{dt} = \frac{1}{C_u}\left[\frac{2\gamma}{3}(C_{uo}^3 - C_u^3) - G(t - t_{\ell o})\right] \tag{53}$$

Thus, for $\tau \to \tau_1 = (k_1\,\epsilon)^{-1}$, the solution of eqn. (53) or (52b) is for x_x^+/ϵ, i.e., $x_s^+ = \epsilon\, x_{s1}$. Then $C_u = C_{uo} + O(\epsilon)$, and eqn. (53) reduces to eqn. (50b). On the other hand, if $\tau \to \tau_2 = k_2\epsilon^2$, $t_{\ell o} = O(\epsilon)$ and eqn. (53) reduces to eqn. (50a), with $x_s^+ = O(1)$. Therefore, the unified solution suggested here is given by eqns. (4), (5a) - (5f), (51), and (52), with eqn. (53) replacing eqn. (52b) for the specific problem considered here.

An indication of the relationship between calculations carried out using case (1), case (2), and case (3) solutions, is given in figures 8 and 9. In figure 8, case (1) (eqns. (6) and (50b))and case (3) (eqns. 52) computations for shock position are compared for $\tau = 20$, $\epsilon = 0.05$ (i.e., $k_1 = 1$ in case (1)). In figure 9, case (2) and case (3) computations for shock position and shock velocity are compared for $\tau = 400$, $\epsilon = 0.05$ (i.e., $k_2 = 1$ in case (2)). In figure 9, the difference in shock velocities is entirely due to the difference between G(t) and $G(t-t_{\ell o})$ and thus gives an indication of the effect of carrying t_ℓ in G in case (3),

i.e., $t_{\ell o} \geq t_{\ell}$. In each comparison, case (3) is considered to be the more accurate calculation, which reduces to the case with which it is being compared, as $\epsilon \to 0$. It should be noted that as τ increases in value to the point that the difference in u, say, between values found using t_{ℓ} in G and not using t_{ℓ} in G, becomes of order ϵ^3, then t_{ℓ} should be neglected; i.e. in the solutions, terms of order ϵ^3 have been neglected, so a term of this order should not be carried as a correction to G(t).

In summary, then, it is possible to construct a unified computational scheme from which numerical results may be obtained for a large range of ϵ and τ values. These solutions are valid in the so called slowly varying time regime, which covers a range of characteristic times, for impressed pressure oscillations, of considerable technical interest.

Large Amplitude Shock Wave Motion

As indicated previously, when $\tau = O(\epsilon^2)$ (case (2)), the shock motion resulting from pressure oscillations impressed downstream of the shock wave, has an amplitude of order unity. As a result, there are conditions under which the shock will move upstream through the nozzle, disappear upstream, and then reappear as the downstream plenum pressure drops to the point where a shock wave in the channel is necessary to satisfy this instantaneous pressure requirement. The conditions for this occurrence and the subsequent shock wave motion depend in a complex manner upon the amplitude of the forcing function,

G, the steady state condition about which the oscillations occur, represented by C_{2d}, the wall shape, f(x), and the numerical value of the time constant, represented by k_1.

The equation which governs the shock motion, repeated here for convenience, is eqn. (47), or in the form suited to the problem under consideration, eqn. (50a).

$$\frac{4k_2}{(\gamma+1)} \frac{dx_{so}}{dt} = -\frac{1}{C_u}\left[C_{2d} + \frac{2\gamma}{3} C_u^3 + G(t)\right] \tag{47}$$

$$\frac{4k_2}{(\gamma+1)} \frac{dx_{so}}{dt} = \frac{1}{C_u}\left[\frac{2\gamma}{3}(C_{uo}^3 - C_u^3) - G(t)\right] \tag{50a}$$

where, since $x_s = x_{so} + O(\epsilon)$, then to the order considered here, x_s and x_{so} are interchangeable. The interesting point indicated by the existence of these equations is that in spite of the fact that signals from the impressed disturbances reach the shock wave "instantaneously," that is there is no lag time in the pressure or velocity solutions for example, the shock wave does not respond instantaneously. The shock velocity is finite, and indeed there is a lag between the impressed disturbance, G(t), and the resulting stretched shock velocity dx_{so}/dt, due to the other terms in the equation. Thus, in equation (50a), for example, it is seen that the term $(C_{uo}^3 - C_u^3)$ always has a sign such that its effect is to cause the shock to move toward the equilibrium or steady state position. On the other hand, G(t) is a forcing function which changes sign periodically. The result is a shock motion which lags G(t).

It is clear from eqn. (47) or (50a) that singularities occur as the shock wave approaches the throat, and $C_u \to 0$. The behavior of integral curves which cross the **axis,** $x_{so} = 0$, on the x_{so} - t plane can be found for a sinusoidal G(t) by writing eqn. (47) for x_{so} (and thus C_u) small compared to unity and for $t - t_o \ll 1$, where t_o is the value of t at which the bracket on the right hand side of eqn. (47) goes to zero at the throat, $x_{so} = 0$. Thus, if, for example,

$$G = G_o \sin bt \tag{54}$$

then

$$\sin bt_o = - C_{2d}/G_o \tag{55}$$

and eqn. (47) becomes, for $x_{so} \ll 1$ and $t - t_o \ll 1$,

$$\frac{dx_{so}}{dt} = - \frac{(\gamma+1)}{4k_2} (b\, G_o \cos bt_o)\left(\frac{t-t_o}{C_u}\right) \tag{56a}$$

$$\cos b t_o = \pm \sqrt{1 - (C_{2d}/G_o)^2} \tag{56b}$$

where, again, $C_u = u_{1u}(x_{so})$ is the value of u_1 at x_{so}, upstream of the shock, and where $C_u^3 \ll t - t_o$. In the neighborhood of the throat, a parabolic wall shape is representative of actual practice. Thus, a typical wall shape and the corresponding solution to eqn. (56) are, in the neighborhood of the throat,

$$f(x) = a x^2 \tag{57a}$$

$$x_{so}^2 = - \frac{(\gamma+1)^{3/2}}{2^{5/2} k_2} \frac{b}{\sqrt{a}} G_o (\cos b t_o)(t-t_o)^2 \tag{57b}$$

Thus, if $\cos bt_o > 0$, the point $0, t_o$ is a center and the integral curves (ellipses) in the neighborhood of this center cross $x_{so} = 0$ with an infinite slope. Such curves are shown in figure 10. On the other hand, if $\cos bt_o < 0$, the integral curves in the neighborhood of $0, t_o$ are hyperbolae, the point being a saddle point, as illustrated in figure 10, and the two integral curves pass through the point $0, t_o$ with slopes

$$\frac{dx_{so}}{dt} = \pm \left\{ \frac{(\gamma+1)^{3/2}}{2^{5/2} k_2} \frac{b G_o}{a^{1/2}} |\cos bt_o| \right\}^{1/2} \tag{58}$$

An understanding of the possible shock motions may be gained by analyzing the integral curves which pass through the saddle points. The three possible configurations for these curves are sketched in figure 11. In these sketches, the arrows indicate the direction the solutions must follow as time increases. In figure 11a, conditions are such that the integral curves entering the saddle point originate from a particular $x_{so} = x_o$ at $t=0$. Those leaving the saddle begin to rise, then reverse their directions and cross the time axis with vertical slope at some point between the center and the next saddle point. Other integral curves are sketched also, in dotted lines. As indicated in the sketch, the paths traced by the integral curves are repetitive. In figure 11c, the opposite situation exists; the integral curves entering the saddle point begin on the abscissa, between a saddle and a center, with an infinite slope and then change direction and enter the next saddle point. Those curves leaving the saddle never return to the axis $x_{so} = 0$, but asymptotically approach a single periodic curve (for a given C_{2d}).

Those curves which originate with an x_{so} greater than any x_{so} on this periodic curve will approach the periodic curve asymptotically from above. This periodic curve is nearly symmetric about x_o, the steady state value of x_{so}. In the dividing case, shown in figure 11b, the curves entering and leaving the saddle points are the same curve.

The integral curve map obtained in any given case depends upon the values of the amplitude of G, C_{2d}, k_2, and the value of dC_u/dx_{so}. Although general solutions from which a general criterion for the dividing condition (figure 11b) could be derived are not available, an approximate result can be found for G as given in eqn. (54) and f(x) as in eqn. (57a). Thus, with these substitutions, eqn. (47) becomes,

$$K x_{so} \frac{dx_{so}}{dt} = - C_{2d} - \Gamma x_{so}^3 - G_o \sin b t \qquad (59a)$$

$$K = \frac{2^{5/2} k_2 \sqrt{a}}{(\gamma+1)^{3/2}} \qquad \Gamma = \frac{2\gamma}{3}\left(\frac{2a}{\gamma+1}\right)^{3/2} \qquad (59b, c)$$

and the slopes of the integral curves at the saddle point are given by eqn. (58). It is assumed that the integral curve which passes through the saddle point at $bt = bt_o$ and also through the next saddle point at $bt = bt_o + 2\pi$ (e.g., see figure 11b), is approximately symmetric about $bt = bt_o + \pi$. At this point, x_{so} is taken to have its maximum value, $(x_{so})_m$, and so $dx_{so}/dt = 0$. Hence, from eqn. (59a),

$$(x_{so})_m = \left(-\frac{2C_{2d}}{\Gamma}\right)^{1/3} \qquad (60)$$

The integral curve in question is approximated by a polynomial,

$$x_{so} = C_1 \tilde{t}(1-\tilde{t}) + 4C_2 \tilde{t}^2 (1-\tilde{t})^2 \tag{61a}$$

$$\tilde{t} = b(t-t_o)/2\pi \tag{61b}$$

which satisfies the conditions that x=0 at $bt = bt_o$ and $bt = bt_o + 2\pi$, and $dx_{so}/dt = 0$ at $bt = bt_o + \pi$. Moreover, at $bt = bt_o$ and at $bt = bt_o + 2\pi$, the correct slopes of the integral curves are obtained if $bC_1/2\pi$ is given by the right hand side of eqn. (58) with the upper sign. Finally, at $bt = bt_o + \pi$,

$$x_{so} = (C_1 + C_2)/4 = (x_{so})_m.$$

Since C_1 and $(x_{so})_m$ are known in terms of the desired parameters, it is necessary now to find C_2, or what is simpler C_2/C_1, where

$$\frac{C_2}{C_1} = \frac{4(x_{so})_m}{C_1} - 1 \tag{62}$$

The desired relation is found by integrating eqn. (59a), over the period bt_o to $bt_o + 2\pi$. The result is, using eqn. (61b),

$$\int_0^1 x_{so}^3 \, d\tilde{t} = -\frac{C_{2d}}{\Gamma} \tag{63}$$

If eqn. (61a) is used in evaluating eqn. (63), and C_2/C_1 is replaced, using eqn. (62), the following cubic equation and solution are found for $(x_{so})_m/C_1 = B$, say,

$$(4B-1)^3 \frac{16}{3\cdot 7\cdot 11\cdot 13} - \frac{1}{2} B^3 + (4B-1)^2 \frac{4}{3\cdot 7\cdot 11} + (4B-1)\frac{2}{3\cdot 5\cdot 7} + \frac{1}{4\cdot 5\cdot 7} = 0 \tag{64a}$$

$$B = \frac{(x_{so})_m}{C_1} = 0.19811 \tag{64b}$$

From eqn. (62), after substituting for C_2, C_1, and $(x_{so})_m$, one finds the equation relating G_o, C_{2d}, k_2 and a for the special dividing case illustrated in figure 11b.

$$G_0^2 = C_{2d}^2 + 0.41652 \frac{2k_2^2 b^2}{(\gamma+1)a} \left(- \frac{3C_{2d}}{\gamma} \right)^{4/3} \tag{65}$$

Then for G_o greater than the special value given in eqn. (65), the integral curves shown in figure 11a result, while for G_o less than the special value, those in figure 11c are found.

Example calculations of the integral curves through the saddle points, with the sinusoidal forcing function given in eqn. (54), with parabolic walls as in eqn. (57a), and using the approximate form to calculate the special value of G_o, eqn. (65), are shown in figure 12. The calculations were carried out by numerically integrating eqn. (59a), using eqn. (58) to find an initial condition near $x_{so} = 0$. In the calculations, b=2, k_2=1, a=(γ+1)/2 = 1.2, x_o = 1.5, $C_u = (2f(x)/(\gamma+1))^{1/2}$ and $C_{2d} = -2\gamma C_{uo}^3/3$. In figure 12, the letters a, b, and c, refer to the corresponding cases shown in figure 11. In each case, only the curves through one saddle point are shown; the repetitive nature of the curves at each saddle point is not shown, for clarity. It should be noted that the value of t_o in figure 12, referring to the location of a saddle point, is different for each case. The centers, which also occur at different values of t for each case, are noted in figure 12. With

the parametric values given above, it was found from eqn. (65) that the special value of G_o, which gives the behavior shown in figure 11b, is

$$(G_o)_{sp} = 4.968098 \tag{66}$$

The curve labeled b in figure 12 indicates that this value is quite accurate. The integral curve leaves $x_{so} \simeq 0$, $t-t_o = 0$ and returns to $x_{so} = 0$ very nearly at $t-t_{so} = \pi$; the approximations employed in deriving eqn. (65) appear to be justified. The curves labeled a and c in figure 12 were calculated using $G_o = 5.5 > (G_o)_{sp}$ and $G_o = 4 < (G_o)_{sp}$, respectively. In each of these cases, curves entering and leaving the saddle point at $t-t_o = 0$ are shown, the behavior in each case following that sketched in the corresponding part of figure 11. It should be noted that the solutions shown in figure 12 are for very simple (parabolic) wall shapes, and that no simple way of predicting $(G_o)_{sp}$ for the case of general wall shapes exists. However, these simple calculations, the results of which are shown in figure 12, serve to illustrate the various cases which may occur, as sketched in figure 11, and thus are extremely useful in interpreting results found for more complicated geometries. For such geometries, it is necessary to integrate numerically along an integral curve leaving a saddle point to see which case occurs for the given parameters. Examples of such calculations are shown later.

With the mathematical behavior of the integral curves through saddle points understood, it is possible to interpret the physical behavior of the shock wave in each case. Referring to figure 11a, for any initial

condition which does not lie on an integral curve entering a saddle point (two are illustrated by circles in figure 11a), the shock passes through the throat and disappears upstream. This is seen by following the integral curve in question as time increases; x_{so} goes to zero, for any initial condition, between a center and a saddle point. As time increases, then, a saddle point occurs at $x_{so} = 0$, and an integral curve rises from the saddle point in the direction of t increasing. This means that the back pressure has decreased to the point where a shock wave must form in the channel in order to satisfy the instantaneous pressure requirements. This is seen by writing the pressure at $x = X$, using eqns. (38), (5b), and (39); since $f''(X) = 0$,

$$P_b = 1 - \epsilon\gamma u_1(X) + \epsilon^2\gamma\left[\left(\frac{2\gamma-3}{6}\right) u_1^2(X) - \frac{C_{2d} + G(t)}{u_1(X)}\right] + \ldots \qquad (67)$$

where $u_1(X) < 0$. From eqn. (67), it is seen that the conditions for the back pressure to be that which gives the subsonic solution (no shock waves) with sonic pressure at the throat (upper dotted curve in figure 2) is

$$C_{2d} + G(t) = 0 \qquad (68)$$

But this condition, for the case where G(t) (and hence the pressure) is decreasing, is precisely the condition for the saddle point, as exemplified by eqns. (54) and (55) and the discussion following these equations. The fact that this back pressure requirement must be satisfied instantaneously by a shock forming at the throat is a result of the fact that there is no time lag in the solutions for the velocity, pressure, etc.

As a result, then, the proper behavior for the shock, after it disappears, is to reappear at the time associated with the first saddle point after its disappearance. It then follows the path given by the integral curve through the saddle point and so disappears again, forms again at the throat at the following saddle, etc. Thus, no matter what the initial condition is, the resulting shock motion is associated with the integral curves leaving the saddle points, as shown in figure 13a. For the periods of time between the shocks disappearing upstream and reforming at the throat, the flow is subsonic throughout the channel. If the initial condition should lie on an integral curve entering the saddle point, the shock moves to the throat and moves away again on the integral curve leaving the saddle point. Thereafter, its motion is the same as that shown in figure 13a.

Referring now to the dividing case shown in figure 11b, it is seen that there are several different possibilities for the shock motion, depending on the initial condition, again indicated by circles. If the initial condition lies outside the integral curves through the saddle points, the shock position merely oscillates with time, never going through the throat. If the initial condition lies beneath the integral curves through the saddle points, the shock moves upstream, passes through the throat and disappears; then for the same reasons mentioned in the previous case, it forms at the throat at the time corresponding to the first saddle point after its disappearance. It then follows the integral curves through the saddle points, so that thereafter, it just moves to the throat and never passes upstream; this motion is illustrated in figure 13b.

If the initial condition should lie on an integral curve through a saddle point, the shock position is completely described by integral curves through the saddle points; the shock never moves upstream of the throat.

Finally, referring to figure 11c, there are again several possible initial conditions. If the initial condition lies above the integral curve entering the saddle point, the shock motion approaches a periodic form, never reaching the throat. If it lies on an integral curve below the curve entering the saddle point, it moves upstream through the throat and disappears, forms at the throat at the time corresponding to the first saddle point after its disappearance, and then moves away from the throat and approaches a periodic motion, never approaching the throat again. This motion is shown in figure 13c. Finally, if the initial condition should lie on the integral curve entering the saddle, the shock wave moves to the throat, moves away immediately on the integral curve leaving the saddle point, and approaches the same periodic motion mentioned above.

The numerical examples shown so far (e.g., figure 12) have been for simple wall geometries for which it is possible to derive an approximate relationship between the parameters for the special dividing case shown in figure 11. (Eqn. 65). For general geometries, it is necessary to integrate equation (47) numerically along the integral curves leaving the singularity, using equation (56a) to find starting values near $x_{so} = 0$, to find which case holds. Examples of such calculations, for the same wall shapes used in example calculations for cases (1) and (2) are shown in figures (14) and (15). Figure (14) shows

calculations made for $C_{2d} = 0$, that is, for the case where the steady state solution is that for which the flow goes through sonic velocity at the throat but is subsonic thereafter, with no shock waves. Clearly, the unsteady motion is that illustrated in figure 11a. In figure (15), two examples are shown in which the only parameter varied is the steady state shock position, x_0. Referring to the integral curves through the first saddle points, it is seen that for $x_o = 1.5$, the situation is that illustrated in figure 11c, while for $x_o = 0.75$, it is that illustrated in figure 11a. Also shown in figure 15 are the solution curves from the initial condition to the point where the shock passes through the throat. With these two curves and those leaving the first saddle point, one can find then the resulting shock wave motions corresponding to figures 13a ($x_0 = 0.75$) and (13c) ($x_o = 1.5$).

In summary, the above examples illustrate the remarkably varied shock motions governed by the deceptively simple first order nonlinear equation (47). Only an outline of the possible shock motion histories has been presented here. In view of possible applications to inlet buzz and flutter and surge problems in turbomachinery, it appears that more work is called for in this problem.

(III) SEPARATION IN UNSTEADY FLOW FIELDS

The basic idea behind this proposed work was to attempt to use work done on steady shock wave boundary layer interactions at incipient separation in ascertaining under what conditions such calculations could be used in unsteady flows. That is, by ordering the partial time

derivative terms relative to the important terms retained in the governing equations in the interaction region, it was felt that one could derive the conditions under which these partial time derivative terms may be neglected. In that event, the solutions found for the steady flow could be used for the unsteady flow cases at each instant of time; that is, the boundary conditions are then time dependent, so the unsteady flow solution is given by a series of steady flow solutions, each with different external conditions. After finding these conditions, they were to be tested modestly, by ascertaining if the parameter range in which time derivatives are important contained the case illustrated experimentally by Meier[6]. That is, since Meier's experiments with shock wave induced separation in a nozzle flow showed that the separation point motion lagged the shock wave motion, it was believed that the terms involving partial time derivatives would be important. It has been found, however, that except for extremely small characteristics times associated with the unsteady flow external to the boundary layer, these time derivatives are not important. This can be illustrated by considering the following two dimensionless terms from the equation of motion

$$\frac{\partial u}{\partial T} + u \frac{\partial u}{\partial x}$$

where $u \frac{\partial u}{\partial x}$ is a term found everywhere in the interaction region except in the region nearest the wall. It is of interest here to concentrate on

---

[6] Meier, G. E. A., "Shock Induced Flow Oscillations," AGARD-CP-168, Flow Separation, 1975, pp. 29-1 to 29-9.

a particular region, say the velocity defect layer in the turbulent boundary layer. In this region, it can be shown[7] that $\partial u/\partial x = O(\epsilon^{-1/2})$ where ϵ is the order of the first time dependent term in the velocity evaluated in front of the shock wave. (I.e., $u = 1 + \epsilon C_u(t) + \ldots$). Hence, if $T = \tau t$, then for the condition $\partial u/\partial T \ll u\, \partial u/\partial x$,

$$\tau \gg \epsilon^{3/2} \tag{69}$$

Clearly, this condition is met for all but very small values of $\bar{T}_{ch}$.

Moreover, in evaluating the τ value associated with Meier's[6] experiments, since $\bar{L} = 25$ mm, $\bar{a}^* \cong 340$ m/sec, $\bar{T}_{ch} \cong 4$ msec., and $\epsilon \cong 0.17$, it is seen that $\tau = 57 = O(k_2 \epsilon^{-2})$. Apparently, then the range of τ values covered by his experiments lies in the slowly varying time regime and, indeed, falls into the regime referred to as case (2) in this report. Evidently, then, the time derivatives are not important in this case; the steady solutions should be valid. The variation with time of the distance between the shock wave and the separation point evidently depends on the fact that the shock motion is large and hence the variation in shock wave strength is large enough to cause this variation. In any event, it does not appear that the cause is due to unsteady effects within the interaction region, as originally suspected. This work will be pursued to the point of indicating whether the rather strong time dependence of the distance between the shock wave and the separation point can be predicted using known steady solutions for the

---

[7] Adamson, Jr. T.C. and Messiter, A.F., "Normal Shock Wave-Turbulent Boundary Layer Interactions in Transonic Flow Near Separation", Transonic Flow Problems in Turbomachinery (Eds. Adamson, Jr., T.C., and Platzer, M.F.) Project SQUID Report MICH-16-PU, 1976, pp. 392-414.

shock boundary layer interaction and the case (2) shock wave motion described in section II of this report.

The authors wish to acknowledge the many fruitful discussions held with Professor Messiter during the course of this work. His help was instrumental in understanding the various shock motions described in the section on Large Amplitude Shock Motions and in particular in deriving the approximate analytical condition for the dividing case, eqn. (65).

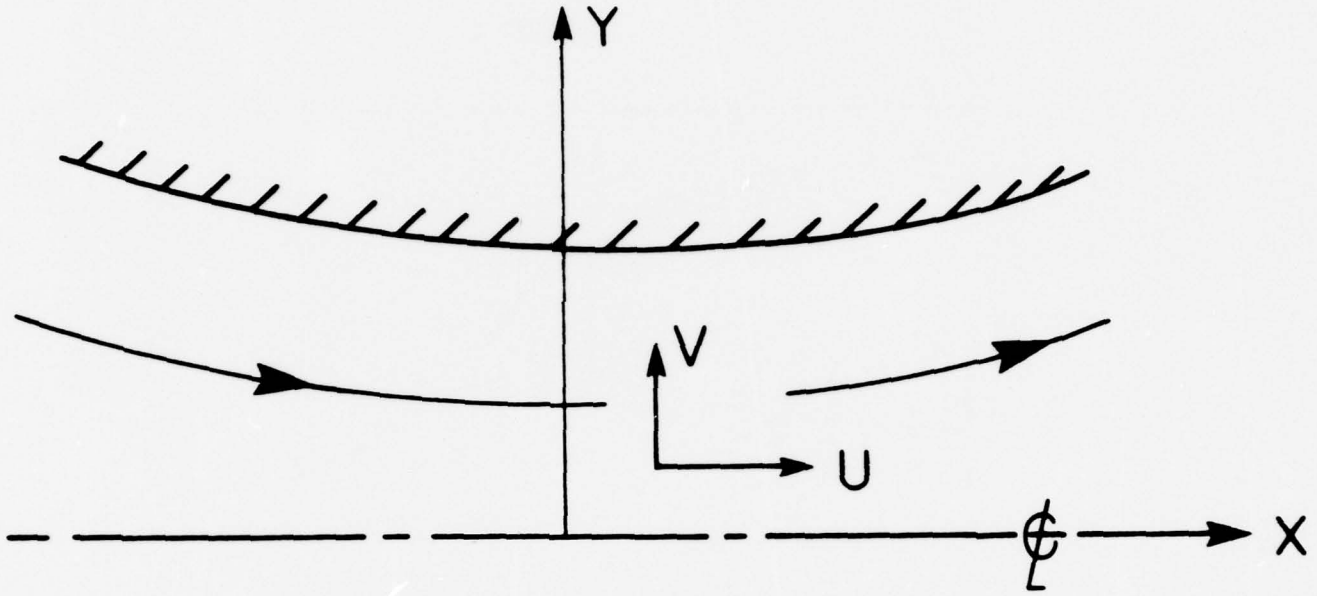

Figure 1. Sketch of symmetric channel flow showing coordinate system and notation used.

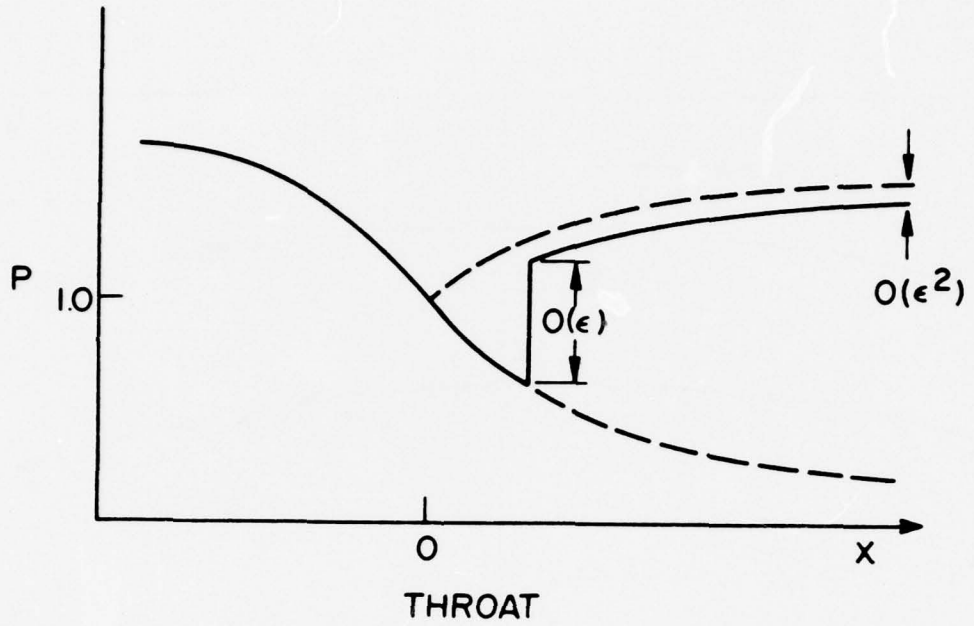

Figure 2. Sketch of pressure distribution in nozzle with accelerating flow. Dotted lines show typical shockless subsonic (upper) and supersonic (lower) distributions downstream of the throat, when the flow is sonic at the throat. Solid line shows distribution when a shock wave exists.

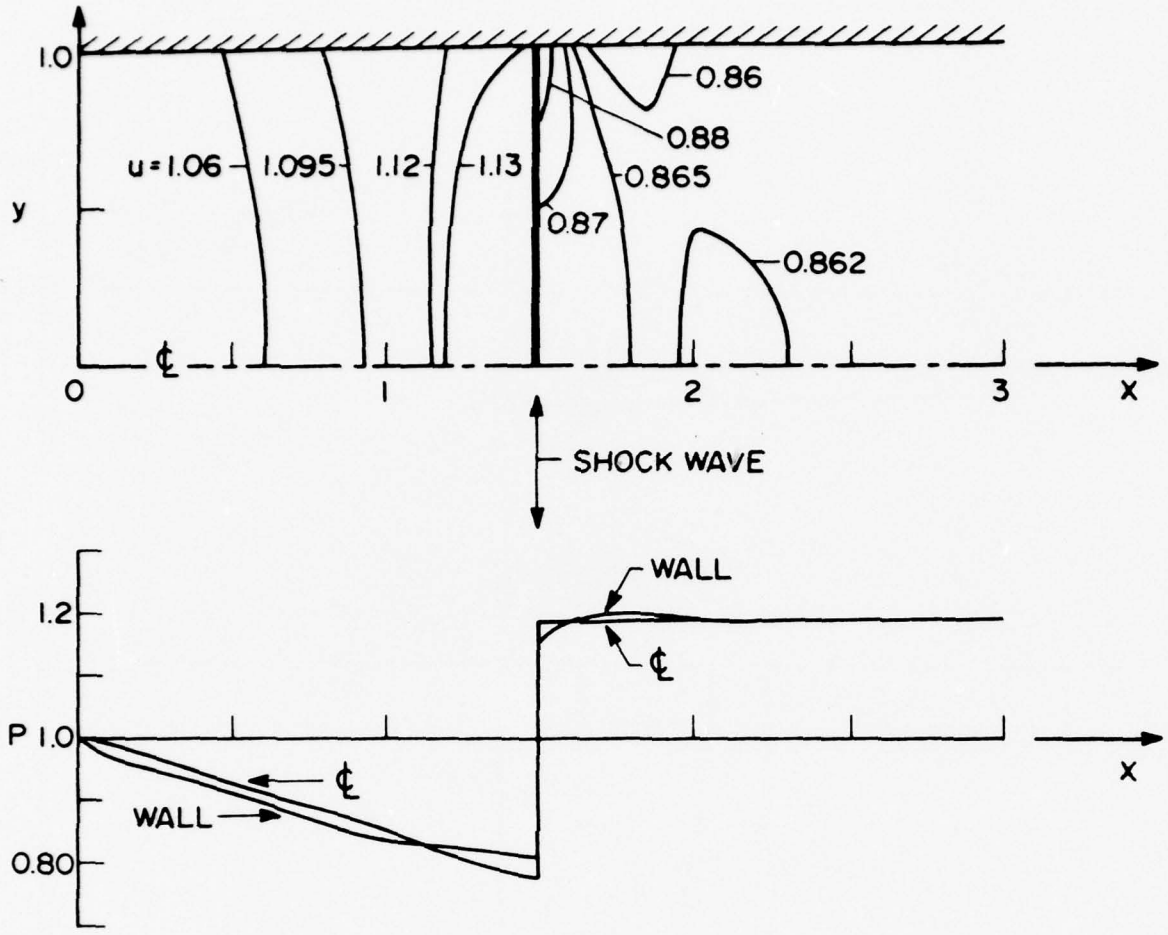

Figure 3. Isotachs and wall and centerline pressure distributions for case (1), for conditions given in equations (9).

(a) t = 0 (steady state)

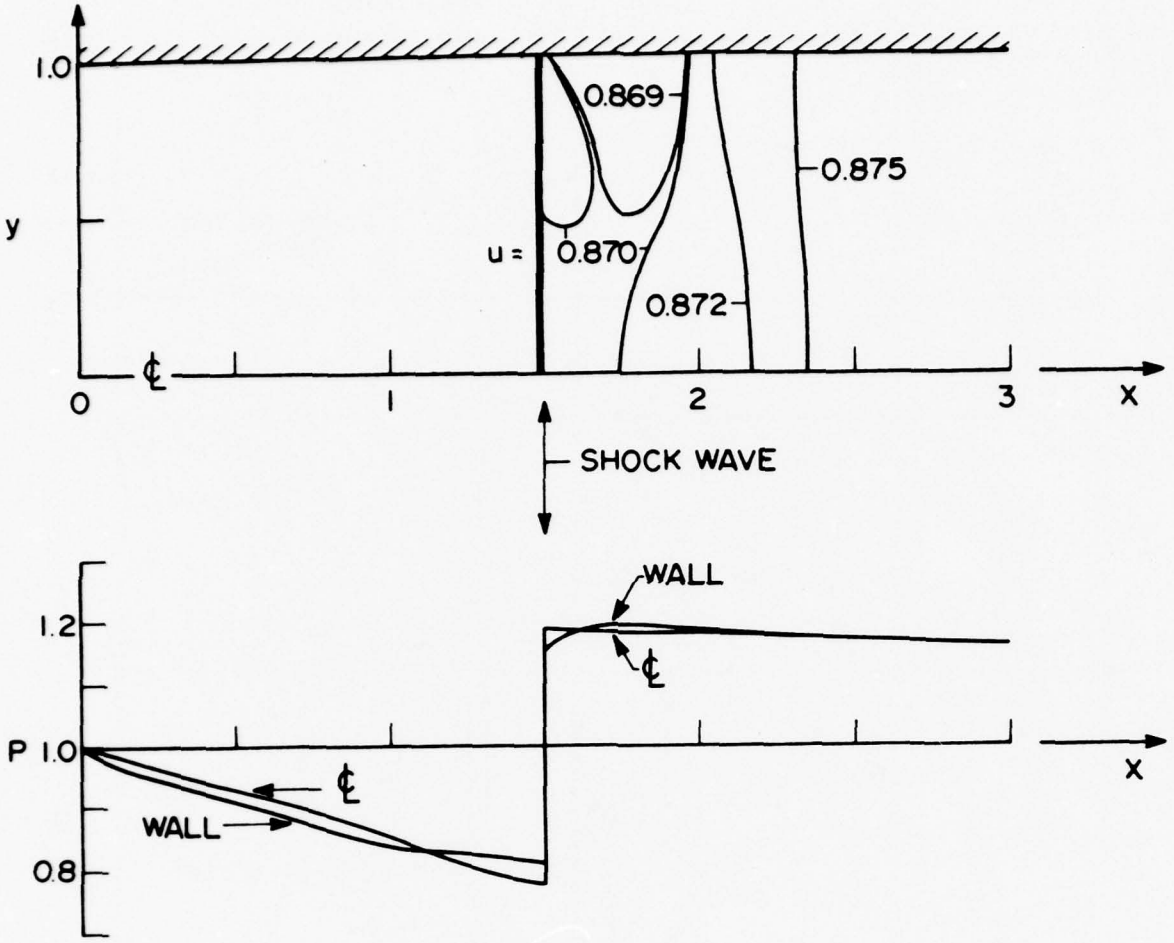

Figure 3. (b) t = 0.39456

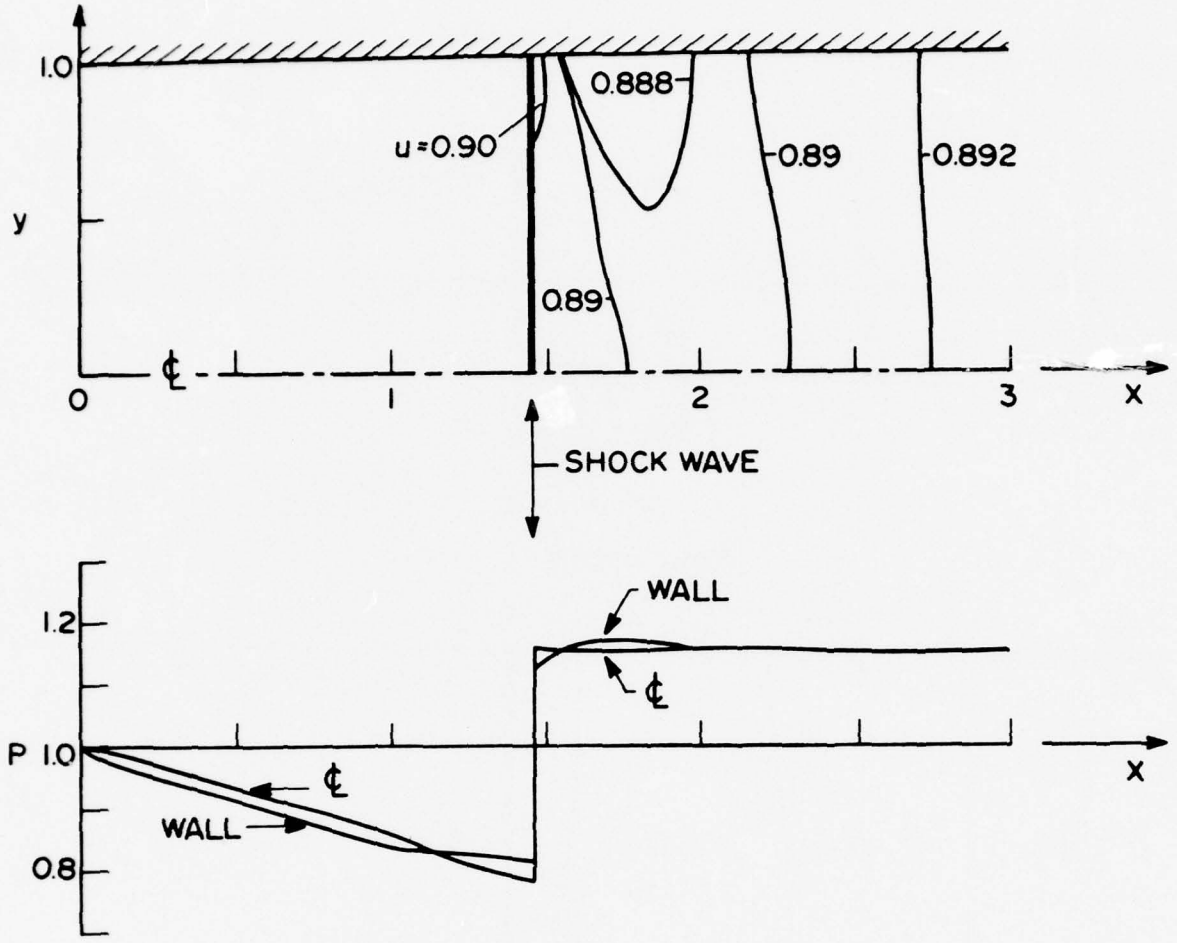

Figure 3. (c) t = 0.78726

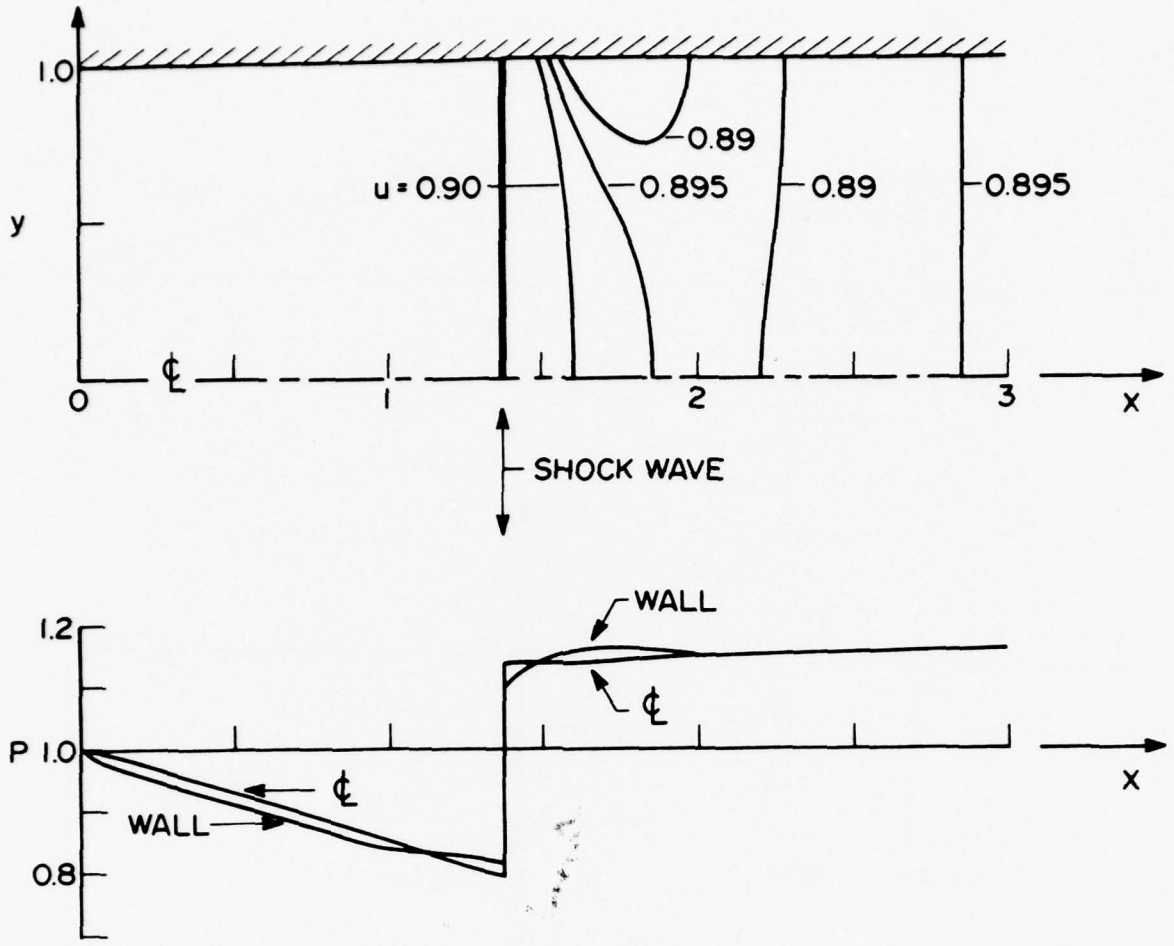

Figure 3. (d) 5 = 1.17996

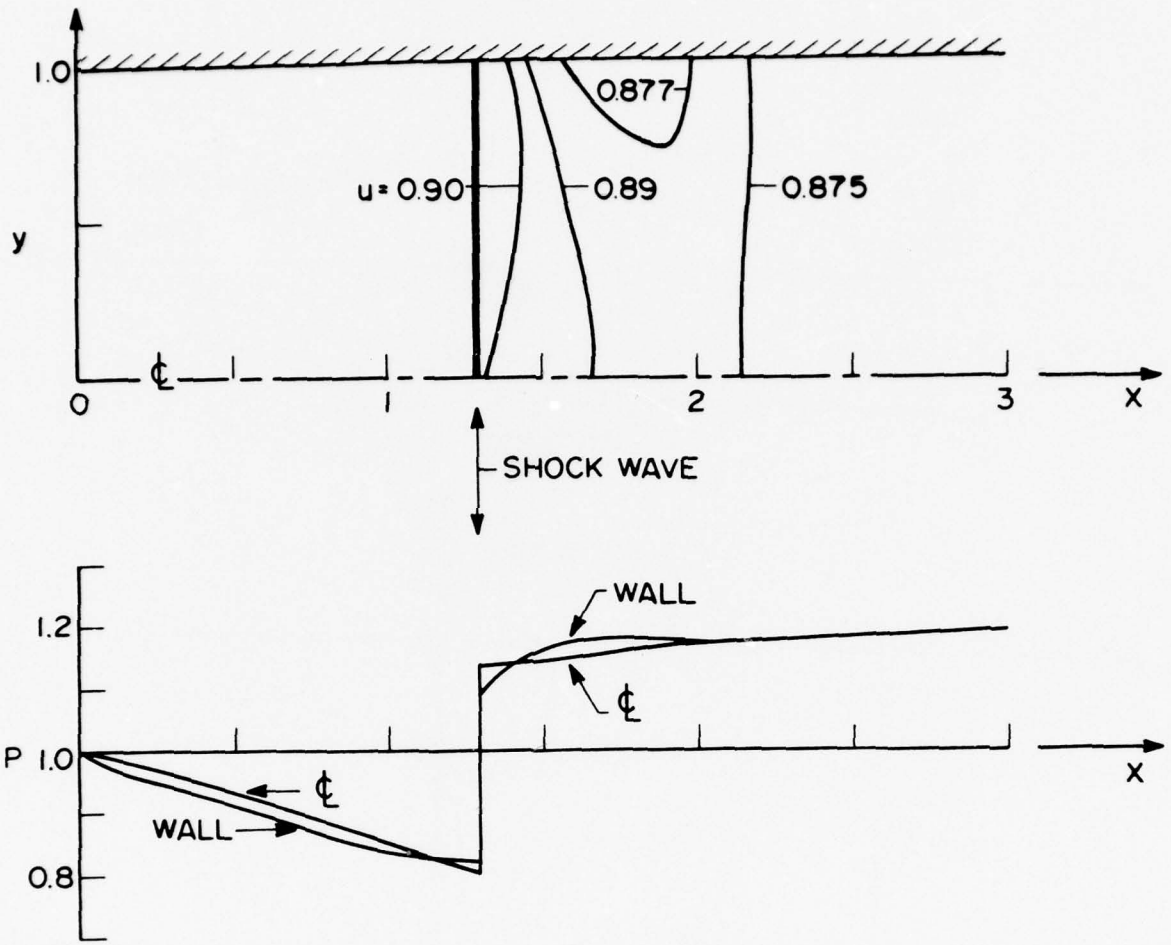

Figure 3. (e) t = 1.57266

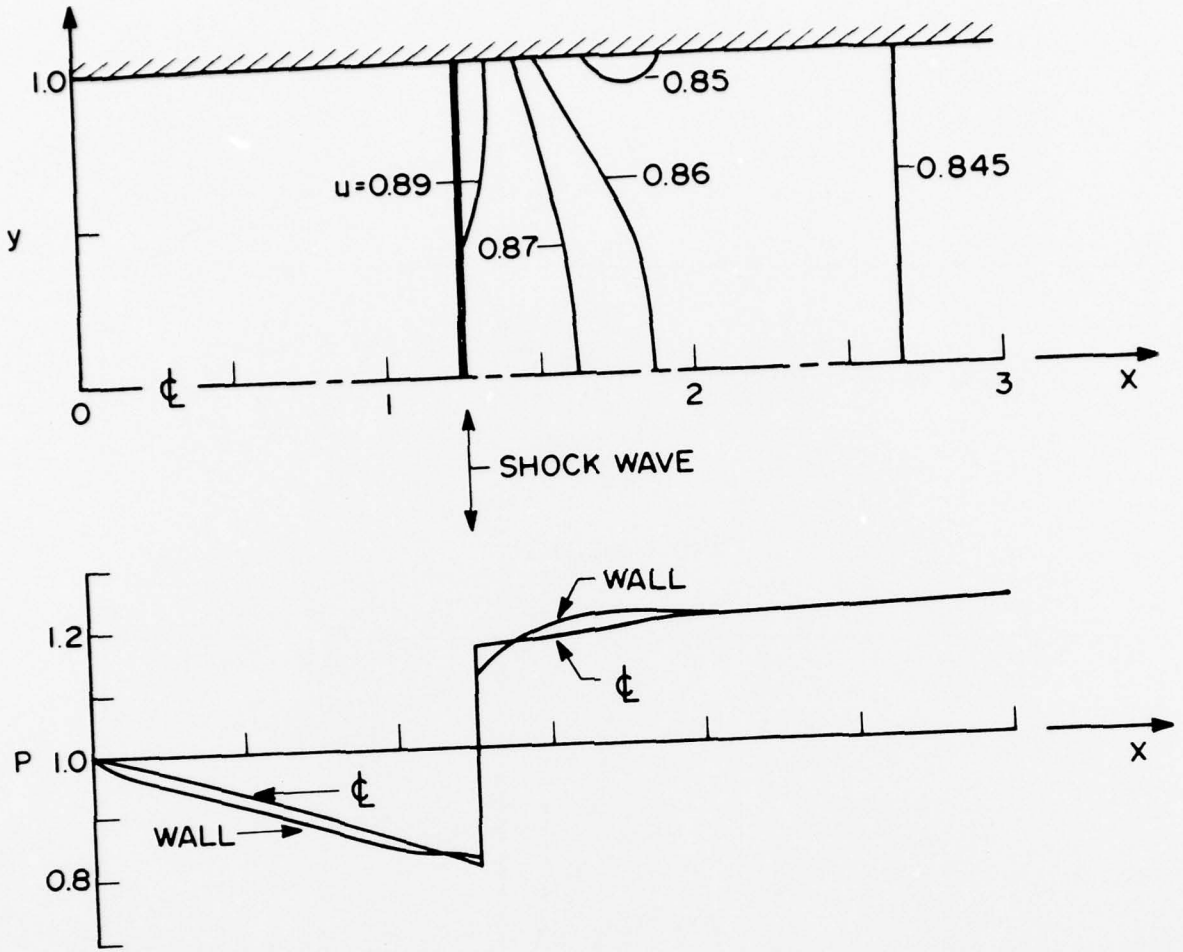

Figure 3. (f) t = 1.96536

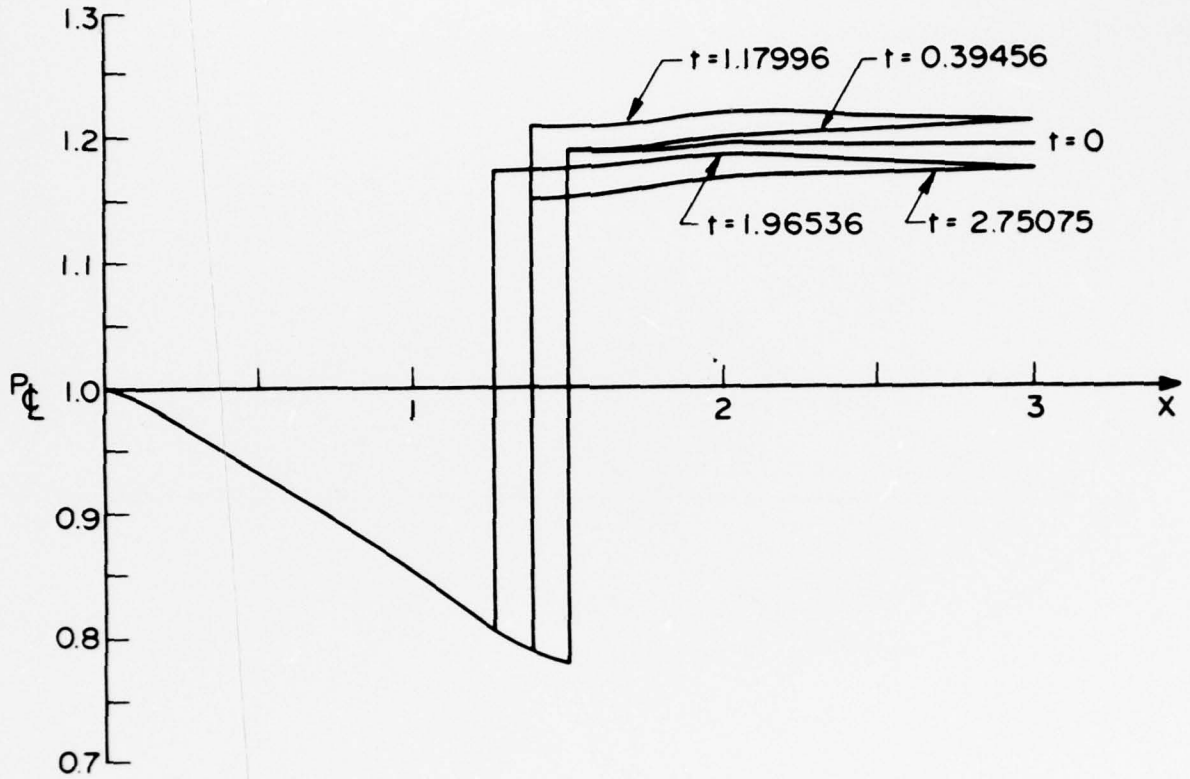

Figure 4. Centerline pressure distributions at various times for case (1) for the same conditions used for figures 3, equations (9).

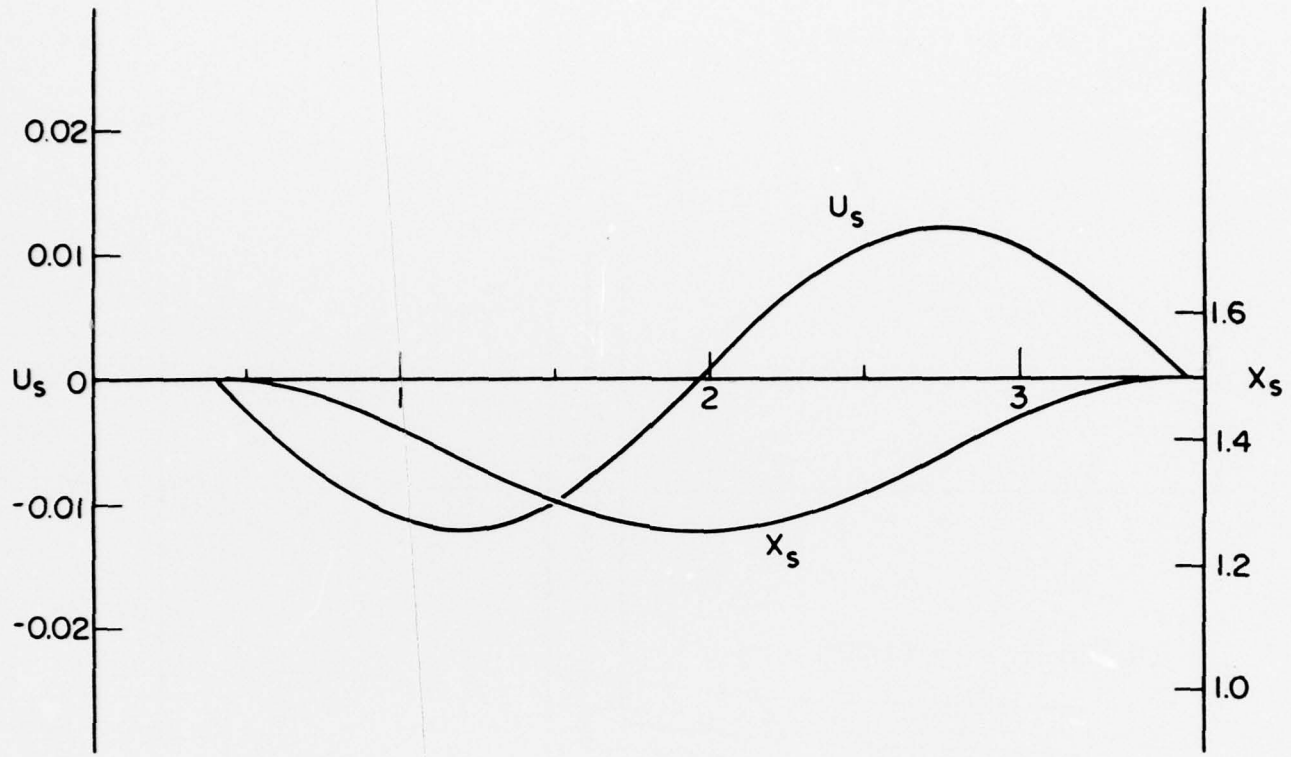

Figure 5. Shock wave velocity, $u_s = k_1 \epsilon^2 dx_{s_1}/dt + \cdots$, and position, $x_s = x_0 + \epsilon x_{s_1} + \cdots$, as functions of time for case (1), for the same conditions used for figures 3, equations (9).

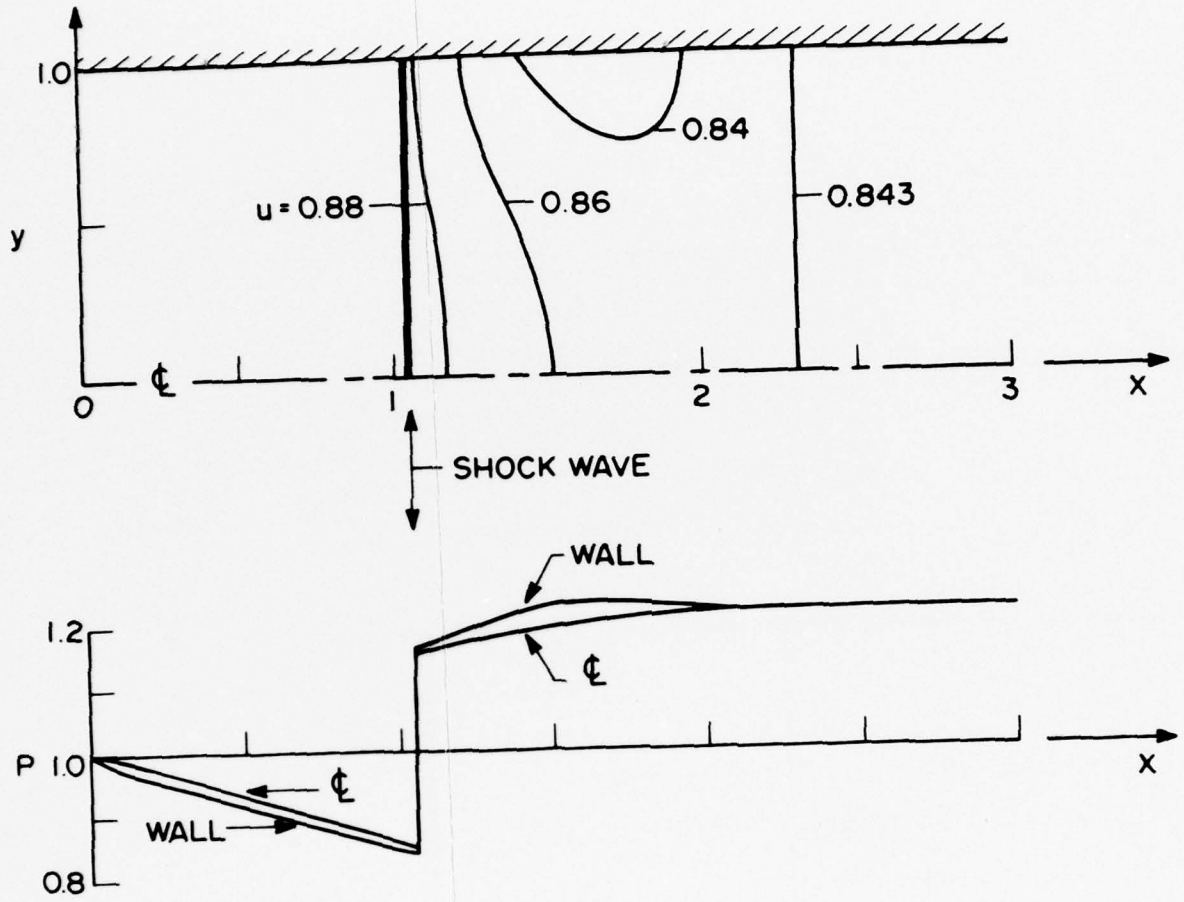

Figure 6. Isotachs and wall and centerline pressure distributions for case (2), for $\tau_2 = 100$ and all other conditions as given in equations (9).

(a) t = 0.7854

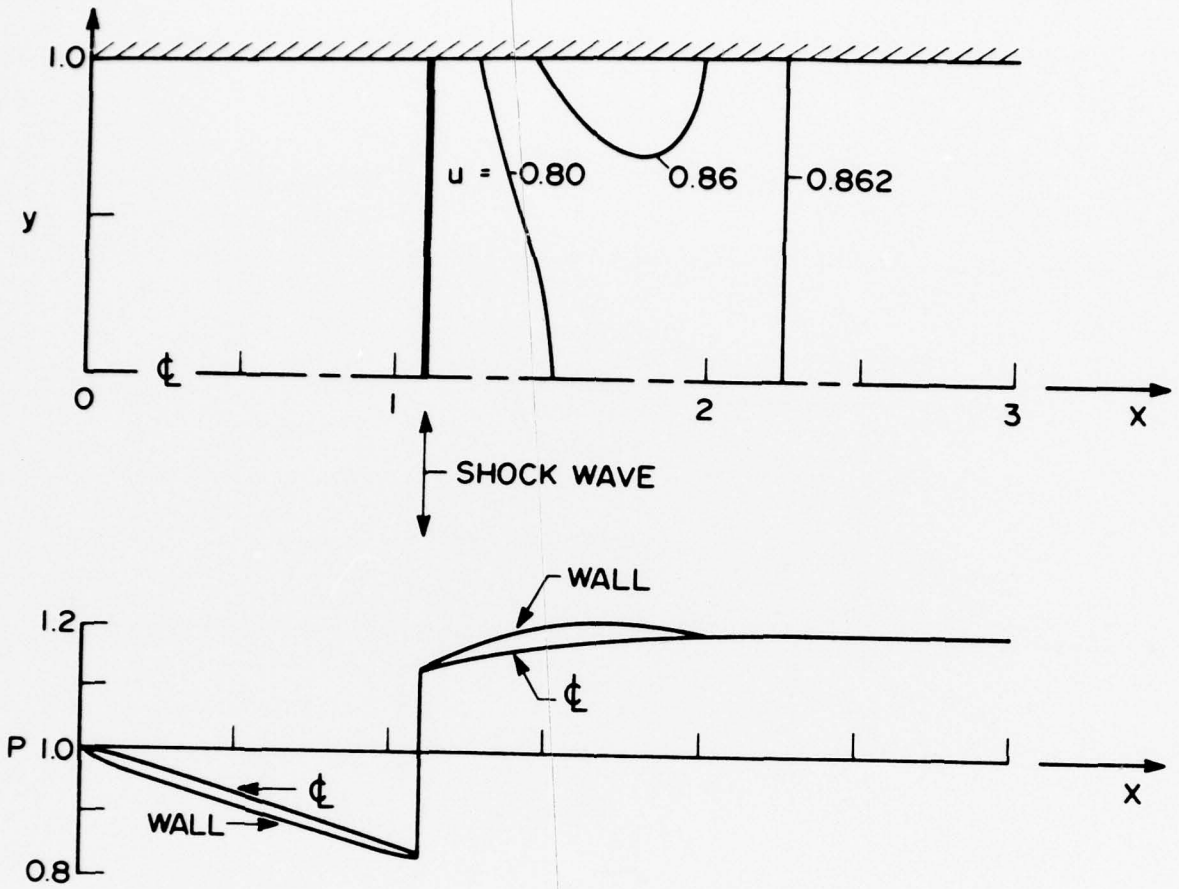

Figure 6. (b) t = 1.57079

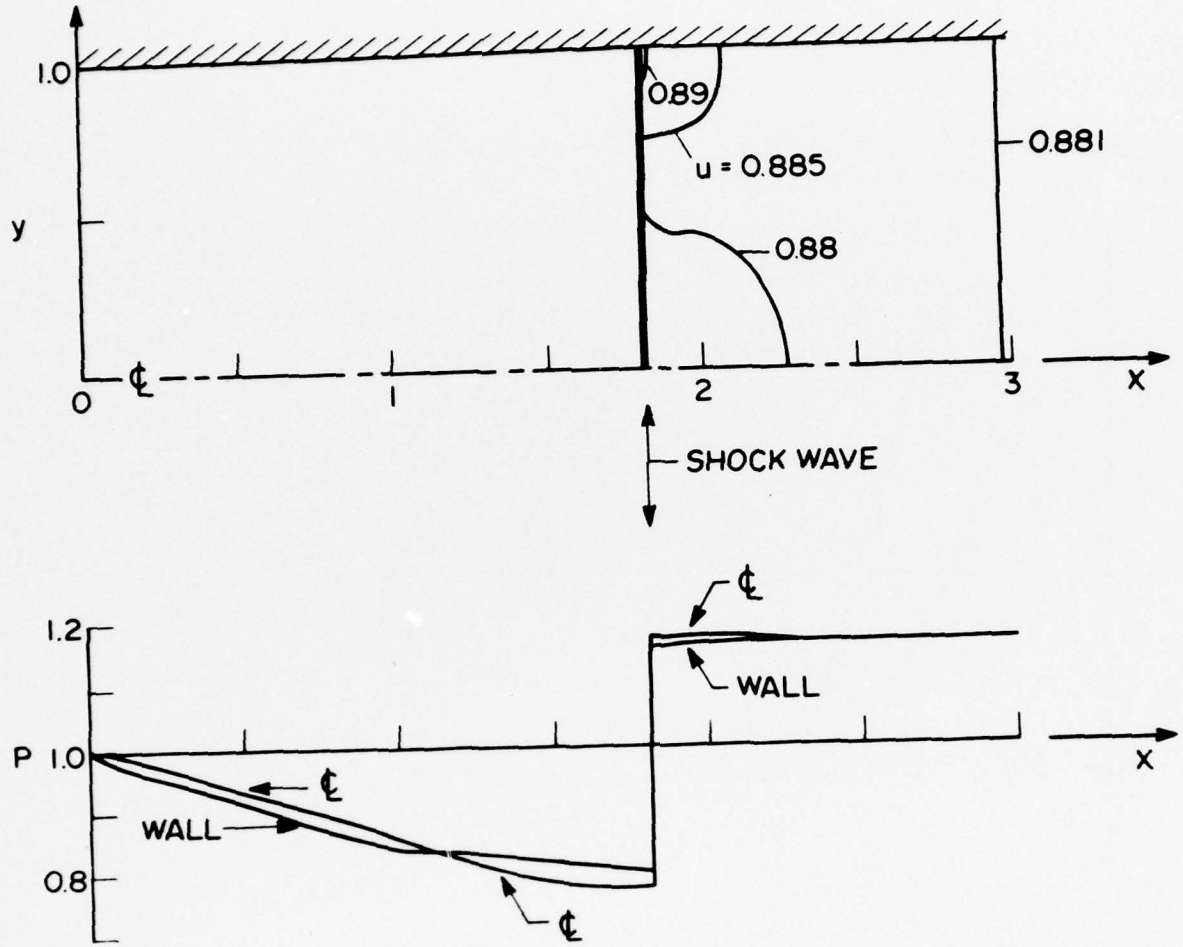

Figure 6. (c) t = 2.35618

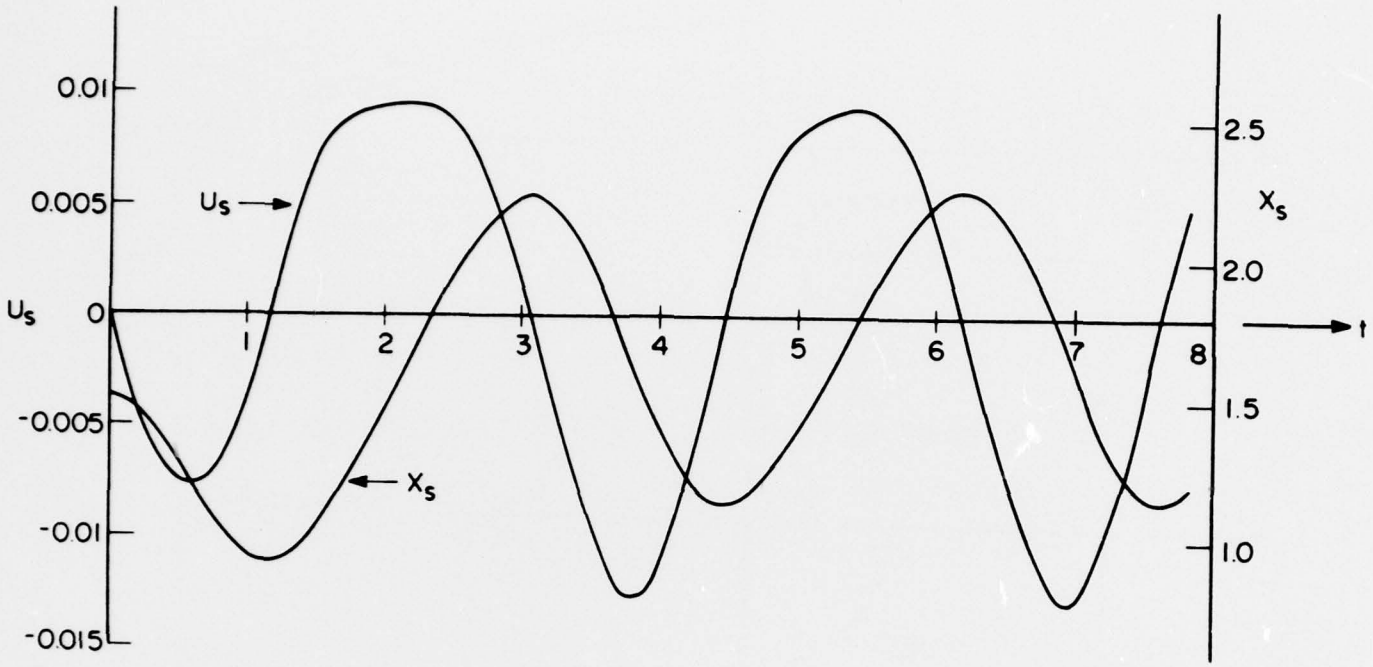

Figure 7. Shock wave velocity, $u_s = k_2\epsilon^2 dx_s/dt$, and position, $x_s = x_{s0} + \cdots$, as functions of time for case (2), for $\tau_2 = 100$ and all other conditions as given in equations (9).

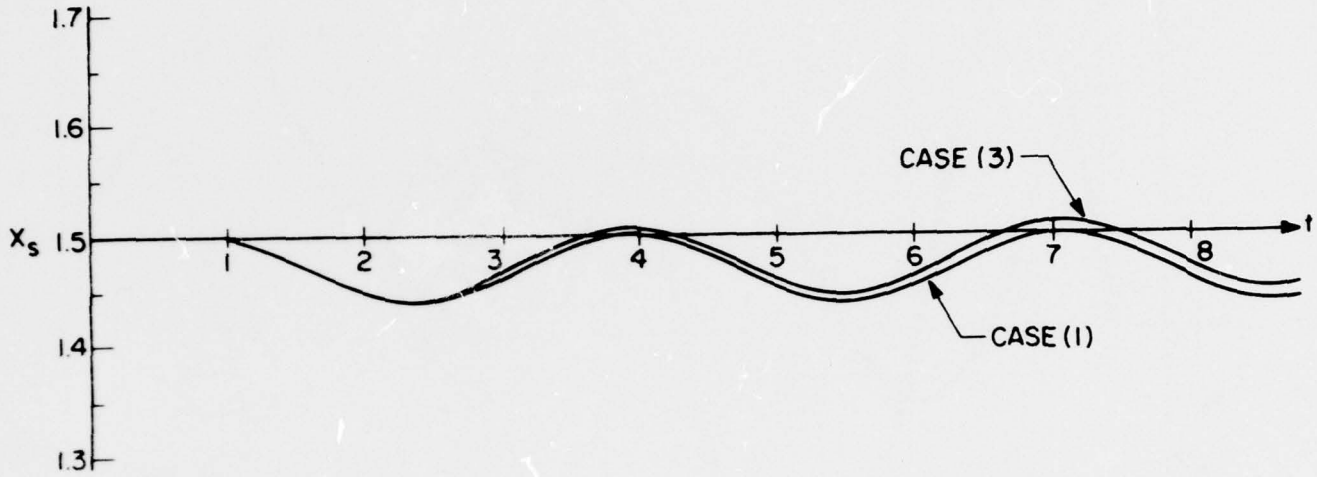

Figure 8. Comparison of case (1) solutions (equations (6) and (50b)) and case (3), unified, solutions (equations (52)) for shock wave position, x_s, for $\epsilon = 0.05$ and all other conditions as in equations (9).

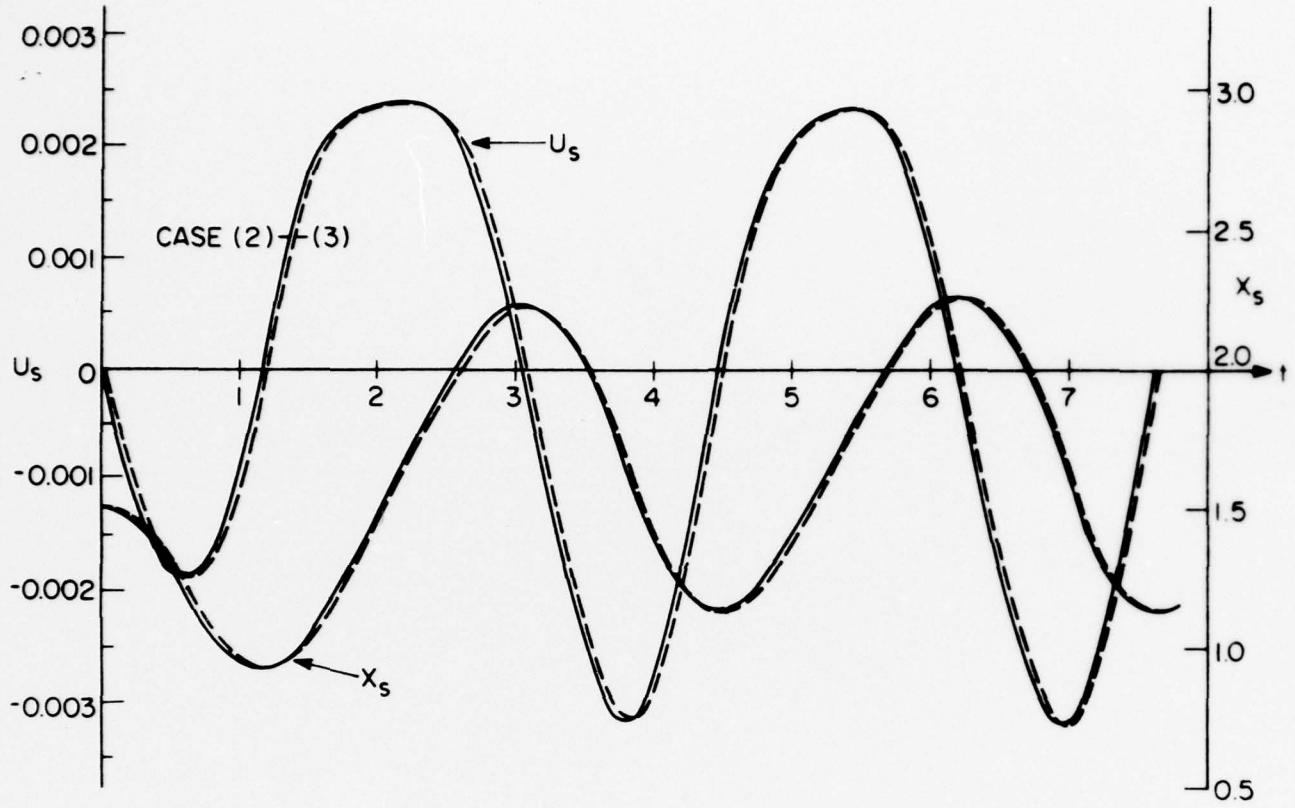

Figure 9. Comparison of case (2) solutions (equations (15) and (50a)) and case (3), unified, solutions (equations (52)) for shock wave position, $x_s = x_{s0} + \cdots$, and shock wave velocity, $u_s = k_2 \epsilon^2 dx_s/dt$, for $\epsilon = 0.05$, $\tau = 400$, and all other conditions as in equations (9). Case (2) solutions are indicated by the solid lines and case (3) by the dashed lines.

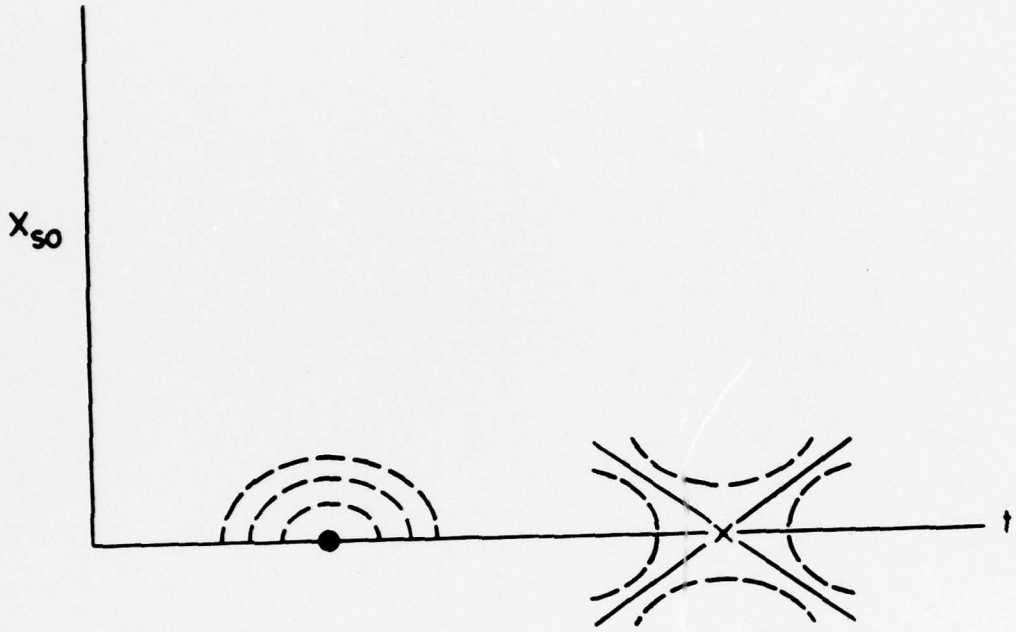

Figure 10. Sketch of integral curves in the neighborhood of a center, •, and a saddle point, x ; solid lines indicate the integral curves which pass through the saddle point.

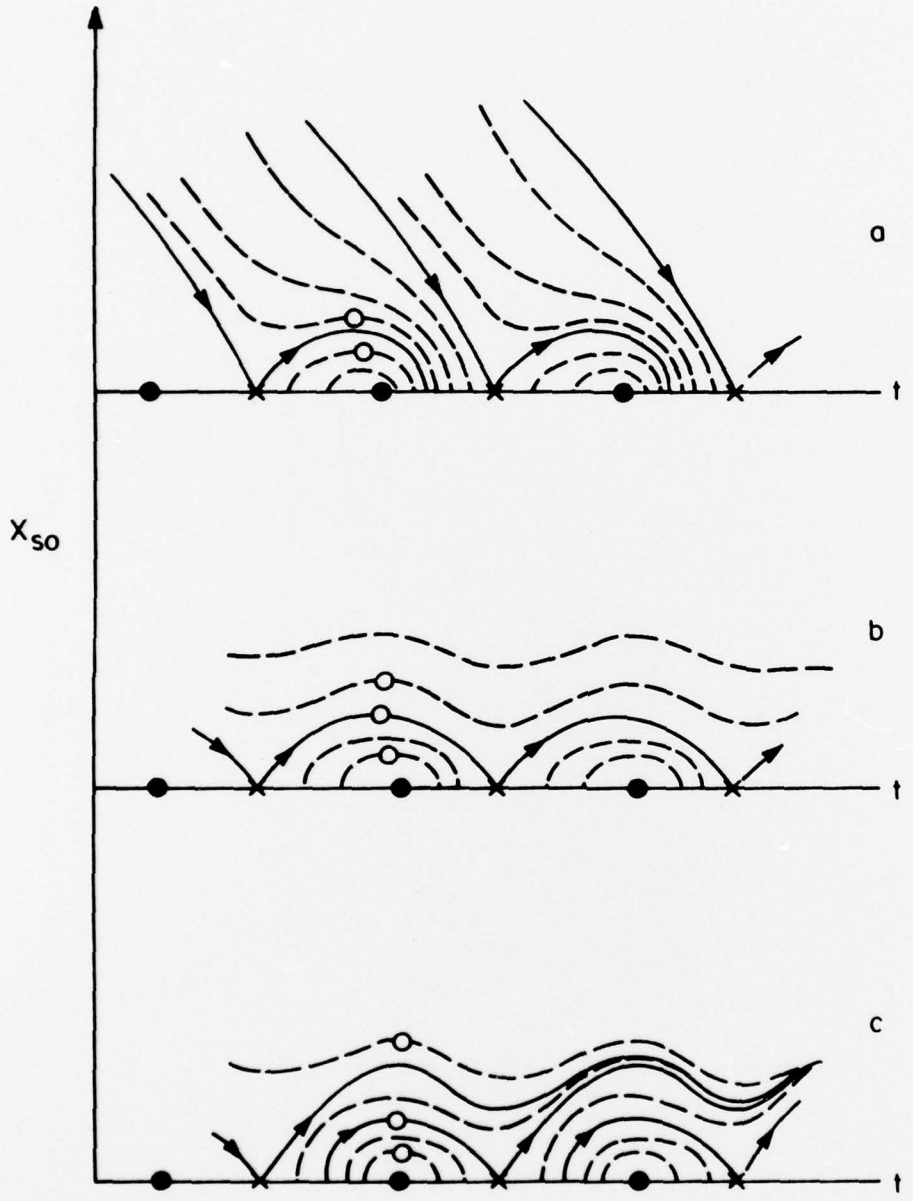

Figure 11. Sketches showing the three possible configurations for integral curves passing through the saddle points (solid lines); other integral curves are indicated by dotted lines. (a) Integral curves leaving the saddle point reach the time axis before the next saddle point. (b) Integral curves leaving the saddle point reach the time axis at the next saddle point. (c) Integral curves leaving the saddle point never return to the time axis.

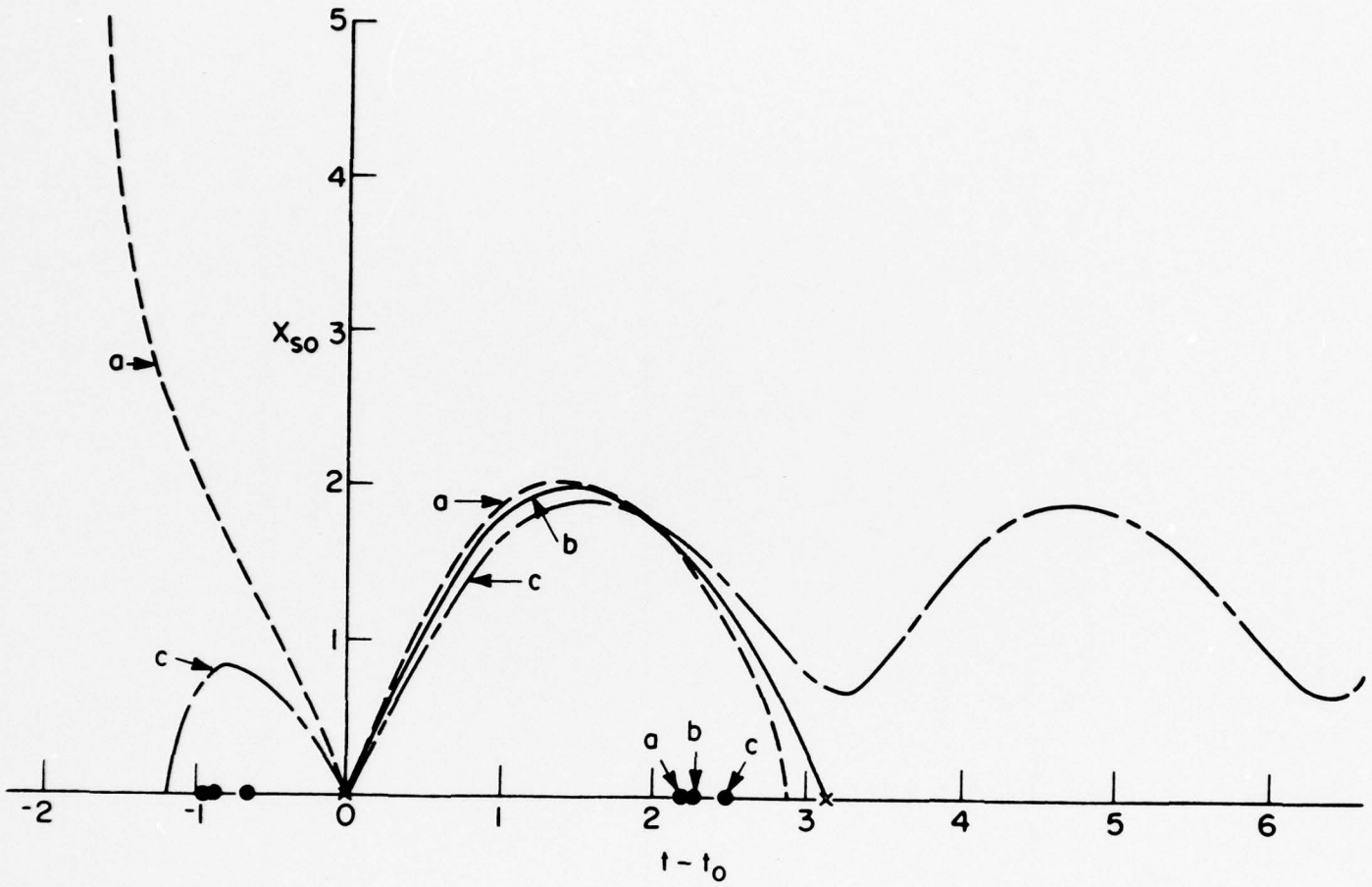

Figure 12. Calculated integral curves for the simple case represented by equations (54), (57a), and (65), with $b = 2$, $k_2 = 1$, $a = (\gamma + 1)/2 = 1.2$, and $C_{2d} = -2\gamma\, C_{u0}^3/3$, illustrating the three cases sketched in figure 11; curves labeled a (---), b (——), and c(-·—·-) refer to the corresponding cases in figure 11. Saddle points are indicated by × and centers by ●.

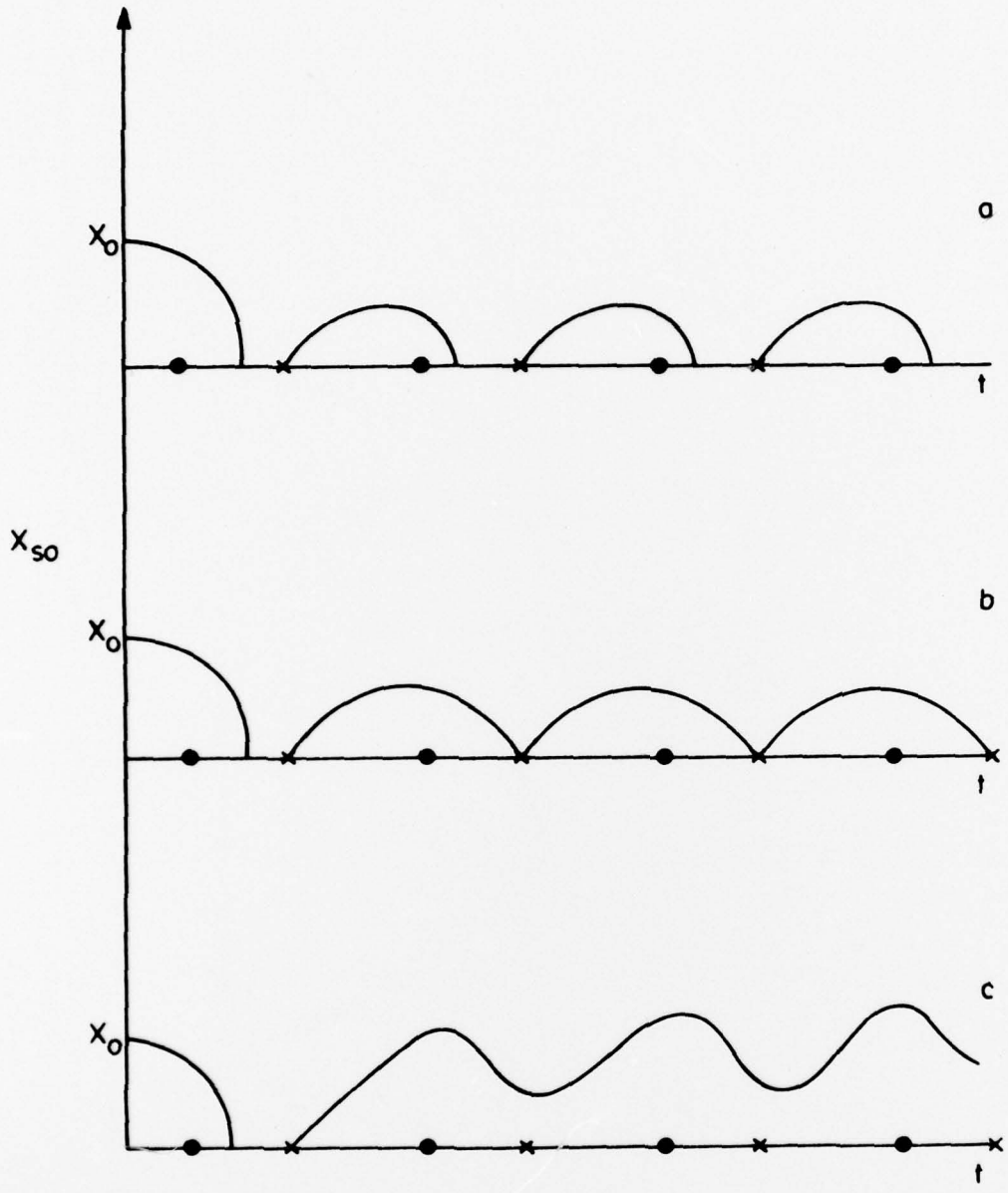

Figure 13. Sketches of shock wave motion when the amplitude of the impressed pressure oscillation is large enough to drive the shock wave upstream of the throat, for each of the three cases shown in figure 11; cases labeled a, b, and c refer to the corresponding cases in figure 11. In each case, x_0 refers to the initial condition for the shock position. (See equation 15.)

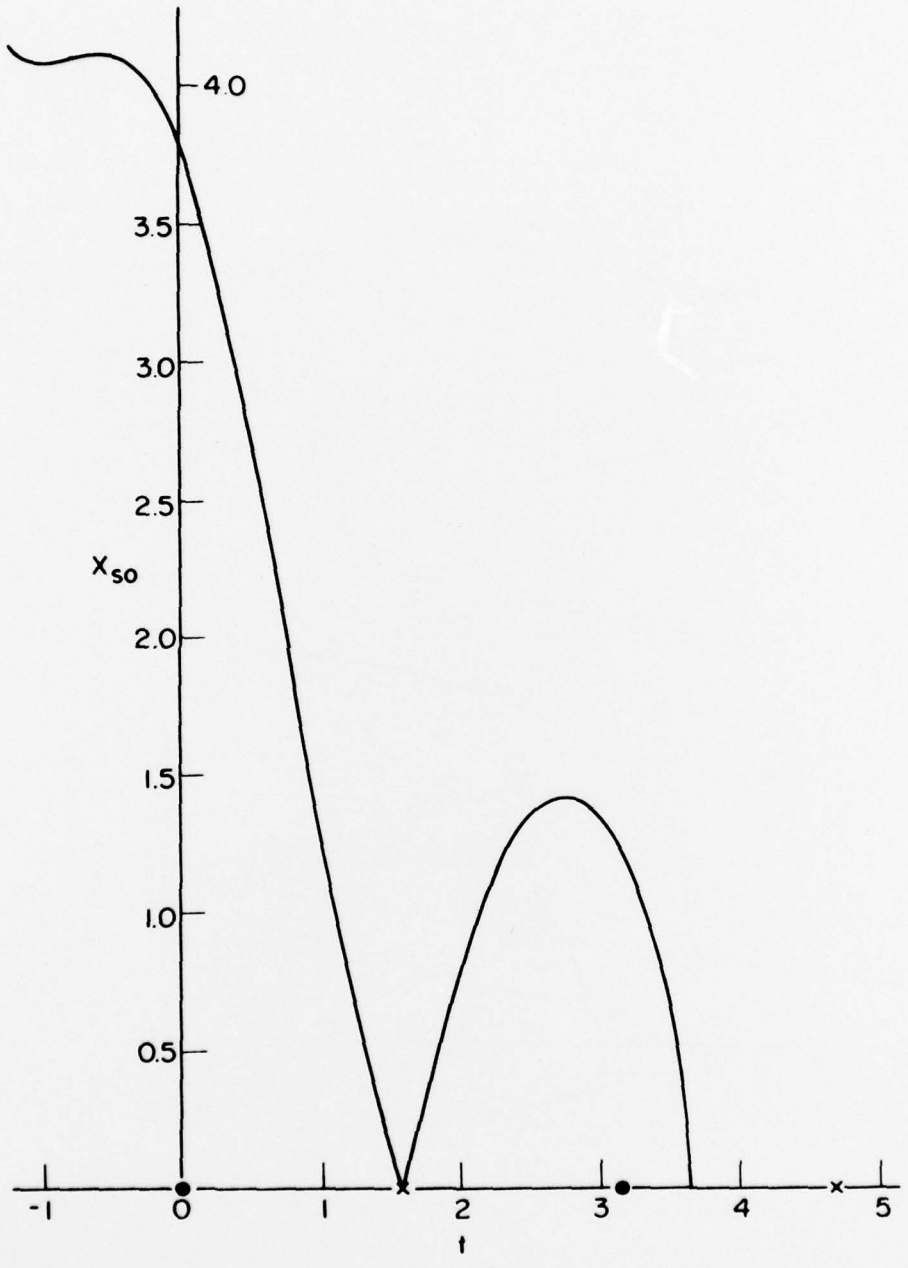

Figure 14. Calculated integral curves through the saddle point illustrating the case sketched in figure 11a, for $C_{2d} = 0$, $G = 4 \sin 2t$, $\gamma = 1.4$, $\tau = 100$, $\epsilon = 0.1$, $C_w = 0$, and f(x) as given in equations (9). Solutions found by numerically integrating equation (47).

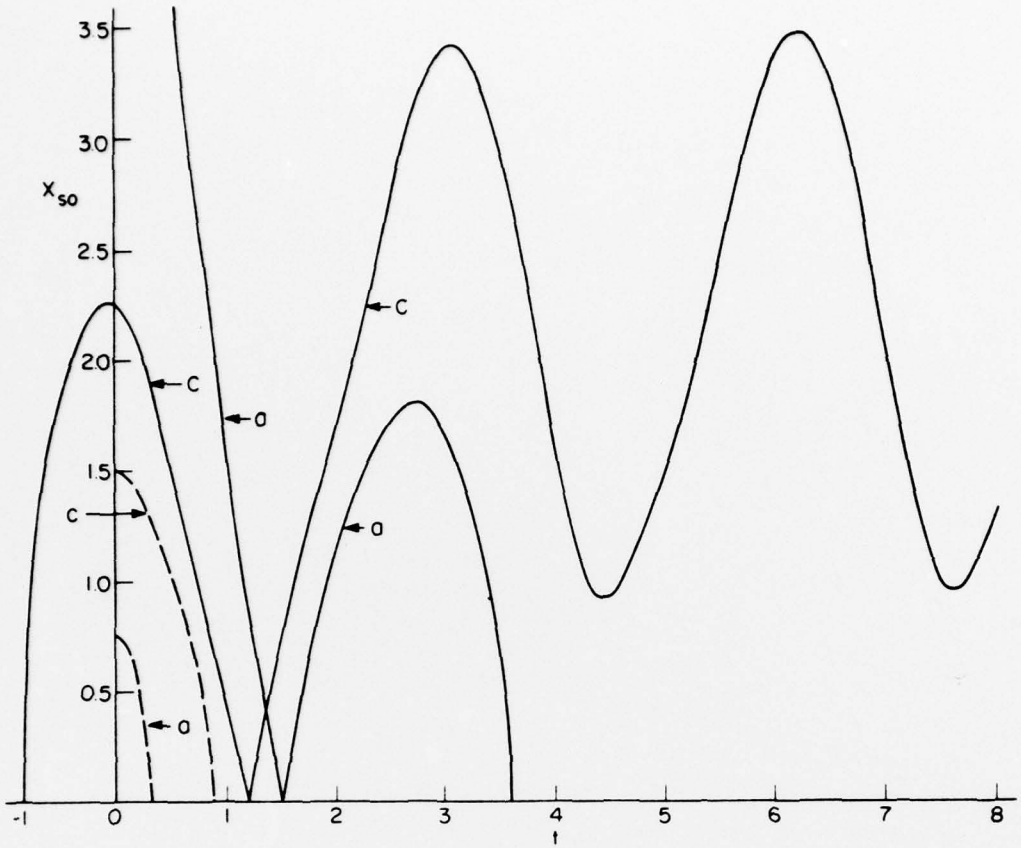

Figure 15. Calculated integral curves through the saddle points (solid lines) and from the initial condition to the time axis (dotted lines) for two values of x_0 and thus C_{2d}. For curves marked a, corresponding to the case sketched in figure 11a, $x_0 = 1.5$; for curves marked c, corresponding to the case sketched in figure 11c, $x_0 = 0.75$. For each case, $G = 4.5 \sin 2t$, $\gamma = 1.4$, $\tau = 150$, $\epsilon = 0.1$, $C_w = 0$, and $f(x)$ is as given in equations (9).

AD-A041 573 MICHIGAN UNIV ANN ARBOR DEPT OF AEROSPACE ENGINEERING F/G 20/4
UNSTEADY MOTION OF SHOCK WAVES IN TWO DIMENSIONAL TRANSONIC CHA--ETC(U)
JUN 77 T C ADAMSON, M S LIOU N00019-76-C-0435
UNCLASSIFIED 014534-F NL

2 OF 2
ADA
041573

END
DATE FILMED
12-78
DDC

SUPPLEMENTARY

INFORMATION

ERRATUM

(replaces pp. 32-35)

UNSTEADY MOTION OF SHOCK WAVES IN TWO DIMENSIONAL TRANSONIC CHANNEL FLOWS

T. C. Adamson, Jr.
M. S. Liou

Department of Aerospace Engineering
The University of Michigan

Final Technical Report

prepared for

Naval Air Systems Command
Contract N00019-/6-C-0435

June 1977

Those curves which originate with an x_{so} greater than any x_{so} on this periodic curve will approach the periodic curve asymptotically from above. This periodic curve is nearly symmetric about x_o, the steady state value of x_{so}. In the dividing case, shown in figure 11b, the curves entering and leaving the saddle points are the same curve.

The integral curve map obtained in any given case depends upon C_{2d}, k_2, G(t), and the wall shape, f(x). Although general solutions from which a general criterion for the dividing condition (figure 11b) could be derived are not available, an approximate result can be found for G as given in equation (54) and f(x) as in equation (57a). Then, equation (47) becomes

$$K x_{so} \frac{dx_{so}}{dt} = - C_{2d} - \Gamma x_{so}^3 - G_o \sin bt \qquad (59a)$$

$$K = \frac{2^{5/2} k_2 \sqrt{a}}{(\gamma+1)^{3/2}} \qquad \Gamma = \frac{2\gamma}{3}\left(\frac{2a}{\gamma+1}\right)^{3/2} \qquad (59b,c)$$

and the slopes of the integral curves at the saddle points are given by equation (58), with t_o and G_o related as in equation (55). Now, if it is assumed that the integral curve which passes through the saddle point at $bt = bt_o$ and also through the next saddle point at $bt = bt_o + 2\pi$ (e.g., see figure 11b) is approximately symmetric about $bt = bt_o + \pi$, then the maximum value of x_{so} is, from equation (59a),

$$(x_{so})_m = (-2 C_{2d}/\Gamma)^{1/3} \qquad (60)$$

Next, if equation (59a) is integrated first over one period (e.g., $bt = bt_o$ to $bt = bt_o + 2\pi$) and then over a half period, then since $x_{so} = 0$ at bt_o and

$bt_o + 2\pi$ and $x_{so} = (x_{so})_m$ at $bt = bt_o + \pi$, one finds the following relations:

$$0 = C_{2d} + \Gamma \int_0^1 x_{so}^3 \, d\tilde{t} \quad , \qquad \tilde{t} = b(t - t_o)/2\pi \tag{61a,b}$$

$$\frac{K x_m^2}{2} = -2 \frac{G_o}{b} \cos b t_o \tag{61c}$$

where, in equation (61c), advantage has been taken of the fact that the integral of x_{so}^3 over half a period is half the integral over a full period because of the symmetry of x_{so}. Substituting for $\cos b t_o$ using equation (55), one finds from equation (61c) the following relation for G_o, for the special case (figure 11b):

$$(G_o^2 - C_{2d}^2)^{1/2} = b K (x_{so})_m^2 / 4 \tag{62}$$

where K is given in equation (59b). Although this equation is useful in setting a first approximation for G_o, a more accurate result may be found by taking into account the fact that the integral curve in question is not in fact symmetric, but is slightly asymmetric. In this calculation, it is necessary to employ an approximate form for $x_{so}(t)$; a cubic equation of the following form suffices:

$$x_{so} = C_1 \tilde{t}(1 - \tilde{t}) + C_2 \tilde{t}(1 - \tilde{t}^2) \tag{63}$$

Now, at $x_{so} = (x_{so})_m$, where $dx_{so}/dt = 0$, $\tilde{t}$ is defined as $\tilde{t}_m$, where

$$\tilde{t}_m = \frac{1}{2} + \delta \tag{64}$$

Also, it is assumed that δ is numerically small enough that terms involving δ^2 may be ignored. Then, from equation (59a) evaluated at $x_{so} = (x_{so})_m$, equation (61a) with equation (63) used in the evaluation of the integral,

equation (59a) integrated over one half period ($\tilde{t} = 0$ to $\tilde{t} = 1/2$) with equation (63) used in integrating the x_{so}^3 term, $(x_{so})_m$ evaluated using equation (63) and equation (64), one can derive the following relations for $(x_{so})_m$, δ, and finally, G_o:

$$(x_{so})_m = (-35\, C_{2d}/16\Gamma)^{1/3} \quad , \quad \delta = 3\, C_{2d}/8\pi\, b\, K (x_{so})_m^2 \qquad (65a,b)$$

$$(G_o^2 - C_{2d}^2)^{1/2} = \frac{b\, K (x_{so})_m^2}{4} - \delta\pi\, (0.207\, \Gamma\, (x_{so})_m^3 - C_{2d}) \qquad (65c)$$

where, again, K and Γ are defined in equations (59b,c).

Example calculations of the integral curves through the saddle points, with the sinusoidal forcing function given in equation (54) and with parabolic walls as in equation (57a), are shown in figure 12; the first approximation to the special value of G_o for case (b), calculated using equation (65c), must be modified using trial and error. The calculations were carried out by numerically integrating equation (59a), using equation (58) to find an initial condition near $x_{so} = 0$. In the calculations, $b = 2$, $k = 1$, $a = (\gamma + 1)/2 = 1.2$, $x_o = 1.5$, $C_u = (2\, f(x)/(\gamma + 1))^{1/2}$, and $C_{2d} = -2\gamma C_{uo}^3/3$, where x_o is the steady state value of x_{so}. In figure 12, the letters a, b, and c refer to the corresponding cases shown in figure 11. In each case, only the curves through one saddle point are shown; the repetitive nature of the curves at each saddle point is not shown, for clarity. It should be noted that the value of t_o in figure 12, referring to the location of a saddle point, is different for each case. The centers,

which also occur at different values of t for each case, are noted in figure 12. With the parameter values given above, it was found that for the special case shown in figure 11b the special value for G_o was, from equation (62), $(G_o)_{sp} = 4.33$ and from equation (65c), $(G_o)_{sp} = 4.77$. The value which gives accurate results (figure 12) is

$$(G_o)_{sp} = 4.968 \tag{66}$$

Thus, equation (65c) is helpful in giving a relatively accurate (4% error) first guess for $(G_o)_{sp}$; in another case, with all other parameters the same, but with $x_o = 0.75$, it was found that equation (65c) gave an estimate with an error of 6%. The curves labeled a and c in figure 12 were calculated using $G_o = 5.5 > (G_o)_{sp}$ and $G_o = 4 < (G_o)_{sp}$, repsectively. In each of these cases, curves entering and leaving the saddle point at $t - t_o = 0$ are shown, the behavior in each case following that sketched in the corresponding part of figure 11.

The solutions shown in figure 12 are for very simple (parabolic) wall shapes. There appears to be no simple way of predicting $(G_o)_{sp}$ for more complicated wall shapes; in general, it is necessary to integrate numerically along an integral curve leaving a saddle point to see which case occurs for the given parameters. Examples are shown later.

With the mathematical behavior of the integral curves through saddle points understood, it is possible to interpret the physical behavior of the shock wave in each case. Referring to figure 11a, for any initial